

INVESTIGATING THE FUNCTIONAL ROLE OF DYSBINDIN-1 (DTNBP-1), A
SUSCEPTIBILITY GENE FOR SCHIZOPHRENIA, IN SYNAPTIC TRANSMISSION.

Lina Marsan

Department of Neurology and Neurosurgery

McGill University, Montreal

A thesis submitted to McGill University in partial fulfillment of the requirements of the
degree of Master of Science in Neurological Sciences

© Lina Marsan

2010

TABLE OF CONTENTS

	PAGE
Abstract (English)	5
Abstract (Français)	6
1. Introduction and statement of the problem	7
1.2 Background	9
2. Experimental design and approach	
2.1 The Sandy mutant mice model	15
2.2 Animal breeding	16
2.3 Fluorescent immunohistochemistry	18
2.4 Modified Golgi-Cox staining	19
2.5 Data analysis	20
3. Results	
3.1 Fluorescent immunohistochemistry	21
3.1.1 Fluorescence intensity of vesicular-glutamate- transporter-1 protein expression	21
3.1.2 Fluorescence intensity of vesicular-glutamate- transporter-2 protein expression	23
3.1.3 Fluorescence intensity of synaptophysin protein expression	24
3.1.4 Fluorescence intensity of syntaxin-1 protein expression	25
3.1.5 Fluorescence intensity of vesicular-GABA-transporter protein expression	26

3.2 CA1 neuronal morphology: Modified Golgi-Cox staining	
3.2.1 Soma size	27
3.2.2 Dendritic arborization	27
3.2.3 Total dendritic length	28
3.2.4 Spine density	28
3.2.5 Spine length	29
3.2.6 Spine surface	29
3.2.7 Spine volume	29
4. Discussion	
4.1 Discussion of pre-synaptic vesicular changes...	29
4.2 Discussion of morphology changes	33
5. Acknowledgement	39
6. References.....	40
Figure 1	58
Figure 2	59
Figure 3	60
Figure 4	61
Figure 5	62
Figure 6	63
Table 1	64
Figure 7	65
Figure 8	66
Figure 9	67
Figure 10	68

Figure 11	69
Figure 12	70
Figure 13.....	71
Table 2	72
7. Appendix	
1a: Functional effect of dysbindin-1 gene on hippocampal oscillation	73
Figure 14	77

Abstract:

Genetic analyses have revealed polymorphisms in dystrobrevin binding protein-1, a gene encoding dysbindin-1, as a potential risk factor for schizophrenia (scz). Whilst significant expression of neuronal dysbindin-1 has been detected pre- and post-synaptically, reduced dysbindin-1 expression, notably in intrinsic hippocampal glutamatergic terminals, were reported in scz postmortem tissues. Thus, suggesting a role of dysbindin-1 in glutamatergic neurotransmission. Using the Sandy mouse model with a natural deletion in dysbindin-1 gene, we investigated whether down-regulation of dysbindin-1 leads to aberrant pre-synaptic changes in hippocampal glutamatergic markers and whether these changes would translate post-synaptically in altered neuronal morphology. We observed a developmental decrease in vesicular glutamate markers and significant alterations in the structure of dendritic spines in homozygous mutants (sdy/sdy) as compared to wild-types. The present study provides the first evidence of a developmental role of dysbindin-1 in synaptic transmission.

Abstract:

Des polymorphismes du gène «dystrobrevin-binding-protein-1», une séquence codant pour la protéine dysbindin-1, sont indicatif du risque potentiel pour la schizophrénie. Bien qu'une significative expression neuronale de dysbindin-1 ait été détectée pré- et post-synaptique, une diminution de dysbindin-1, notamment dans les terminaux glutamatergiques de l'hippocampe, a été rapportée dans les tissus post-mortem de schizophrènes. Ces résultats suggèrent un rôle de dysbindin-1 dans la neurotransmission glutamatergique. Utilisant le modèle de souris Sandy avec une suppression naturelle dans le gène dysbindin-1, nous avons examiné si la diminution de dysbindin-1 est médiateur de changements pré-synaptiques dans le circuit glutamatergique de l'hippocampe et se traduire post-synaptiquement en altération de la morphologie neuronale. Nous avons observé une diminution développementale des marqueurs de vésicules glutamatergiques et des changements significatifs dans la structure des épines dendritiques chez les mutants homozygotes contrairement aux contrôles. Notre étude fournit la première preuve d'un rôle développemental de dysbindin-1 dans la transmission synaptique.

1. Introduction and statement of the problem:

Schizophrenia (scz) is a heterogeneous, chronic and debilitating neuropsychiatric disease affecting individuals in adolescence/early adulthood. This illness has an estimated 0.7% lifetime prevalence (Saha *et al.*, 2005). Patients display a range of mental deficits, including, cognitive decline, emotional disturbances, hallucinations and delusional perceptions that deteriorate their self-care, interpersonal and social skills. A current leading hypothesis suggests that scz is a neurodevelopmental disorder affecting the glutamatergic synaptic functions of cortical and limbic structures whereby disruption of brain development during early period of life would contribute to the emergence of psychosis in adulthood (Weinberger, 1996). While it is generally agreed that both environmental and genetic factors are equally important neurodevelopmental risk factors to this disorder (Tsuang *et al.*, 2001; Sullivan *et al.*, 2003), genetic epidemiological studies point to a significant heritable component (Prescott and Gottesman, 1993). Amongst the array of susceptible genes identified, a number of recent studies have reported an association between scz and single nucleotide polymorphisms (SNP) and/or haplotypes of the dystrobrevin binding protein-1 gene (DTNBP-1; dysbindin-1). Interestingly, analyses of post-mortem brains from patients diagnosed with scz have demonstrated reduction in dysbindin-1 protein and mRNA expression in the hippocampus (Talbot *et al.*, 2004; Weickert *et al.*, 2004), a locus of abnormality in scz (Bilder *et al.*, 1995; Heckers *et al.*, 1998). The attenuation was prominent in intrinsic glutamatergic terminals (Talbot *et al.*, 2004), thereby suggesting a probable role of dysbindin-1 in the hippocampal glutamatergic system. However, the possible mechanism(s) by which the down-regulation of dysbindin-1 mediates the abnormal cortical/limbic glutamatergic synapses in scz is still unknown. Thus, my masters project aimed at addressing the key

question of **how down-regulation of dysbindin-1 protein expression disrupts the normal developmental processes of hippocampal glutamatergic synapses, both pre- and post-synaptically, and its relevance to the generation of scz related**

neurophysiological phenotypes. The general hypothesis of this project was that mice with mutation in DTNBP1 gene (dysbindin-1 knockout mice or Sandy mice) will show an alteration of the pre-synaptic and/or post-synaptic markers of glutamatergic transmission within the hippocampus. In order to test this hypothesis, we followed a systematic approach combining molecular and morphological assessments of the offspring of the Sandy (sdy) mouse. This mouse model has previously been reported to display scz-related behaviors; our group and others have recently shown significant changes in cognitive functions along with differences in hippocampal pre-synaptic glutamatergic transmission (Chen *et al.*, 2007; Bhardwaj *et al.*, 2008; Feng *et al.*, 2008; Cox *et al.*, 2009; Takao *et al.*, 2008; Jentsch *et al.*, 2009). My specific aims were as follows:

Aim 1: To investigate the pre-synaptic changes in hippocampal glutamatergic terminals at pre-pubertal developmental periods using the glutamate specific developmentally regulated pre-synaptic vesicular protein markers vesicular-glutamate-transporter 1 and 2; the ubiquitously expressed vesicular integral membrane protein marker synaptophysin; the pre-synaptic membrane marker syntaxin-1A expressed throughout development. As a positive control for vesicular changes, changes in main inhibitory neurotransmitter GABA will be analyzed via quantifying expression of vesicular GABA transporter. We hypothesized decreases in protein molecular markers specific to vesicular and synaptic glutamatergic markers.

Aim 2: To investigate possible resultant changes in hippocampal CA1 pyramidal neuronal morphology during adulthood. We hypothesized aberration in the morphology and structure of CA1 pyramidal neurons.

My data provides further evidence supporting the role of dysbindin-1 in glutamatergic synapses and shows the importance of dysbindin-1 across early post-natal time frames. These alterations may result in significant changes in neuronal morphology which perhaps contributes to some of the cognitive symptoms (i.e. impaired memory formation) observed in scz. Thus, the sdy mouse model provides important and unique insight into the potential role of the dysbindin-1 gene in the development of this devastating mental disorder.

1.2 Background

Dysbindin-1, a coiled-coil protein encoded by the dystrobrevin binding protein-1 (DTNBP-1) gene, located on chromosome 6p22.3 in humans, was recently discovered in a screen for genes involved in cognitive impairments often associated with Duchenne muscular dystrophy (Benson *et al.*, 2001). The dysbindin family comprises three members- dysbindin-1, 2, and 3, of which only dysbindin-1 locus is reported to be associated with scz (Talbot *et al.*, 2009). Dysbindin-1 has three alternatively spliced isoforms, 1A, 1B and-1C, in humans; but in the mouse only dysbindin-1A (352 amino acid, ~50kDa) and 1C (N-terminal truncated ~33kDa) are expressed. The single prominent protein motif in dysbindin-1 is a 100 amino acid coiled-coil domain (CCD) between N- and C-terminals, that is believed to be involved in protein-protein interactions (for review see Talbot *et al.*, 2009).

Dysbindin-1 is expressed throughout the mouse and human brains (Benson *et al.*, 2001; Benson *et al.*, 2004). Its expression is exclusively confined to neurons with no detectable expression in glia. High levels are detected in a number of regions implicated in cognitive processes, including the hippocampus and prefrontal cortex (PFC; Talbot *et al.*, 2004; Weickert *et al.*, 2004). Hippocampal pyramidal cells have a distinctly higher

level of dysbindin-1 protein in mossy fibre terminals and in the cell body, dendrites and dendritic spines of CA1 and CA2/3 neurons (Talbot *et al.*, 2004; Weickert *et al.* 2004; Talbot *et al.* 2006). Dysbindin-1 is present in both pre- and post-synaptic compartments with dysbindin-1A, the predominant form, highly concentrated in PSD fractions, 1-B in pre-synaptic fractions and 1-C in both.

The neuronal functions of dysbindin-1 protein are not well-understood. In the brain, dysbindin-1 (352 amino acid, ~50kD protein) is a member of the Biogenesis of Lysosome-related Organelle Complex-1 (BLOC-1), a protein complex involved in vesicle/synaptic membrane protein trafficking (Li *et al.*, 2003) and dendritic branching (Chen *et al.*, 2005). It was shown to interact with several other members of this complex such as pallidin, muted and snapin (Nazarian *et al.*, 2006). Furthermore, dysbindin-1 also binds to both α and β -dystrobrevin, components of the Dystrobrevin Protein Complex, a protein complex implicated in synaptic structures and signaling (Benson *et al.*, 2001; Li *et al.*, 2003). Although a handful of recent literature has provided information on its neuronal location, the function of dysbindin-1 in the brain has yet to be fully understood.

An overwhelming number of studies have reported dysbindin-1 as a candidate gene associated with scz (Straub *et al.*, 2002; Kendler *et al.*, 2004; Owen *et al.*, 2004; Williams *et al.*, 2005). The linkage of chromosome 6p22.3 was originally reported by Straub *et al.* (2002) following their pursuit in Irish high-density scz families of a vulnerability locus for scz on chromosome 6p24-22 (Straub *et al.* 1995). The association is not the result of a causative mutation but rather single nucleotide polymorphisms (SNP) and/or haplotypes in the gene (Straub *et al.*, 2002). This association was replicated in the Irish population (van den Oord *et al.*, 2003) as well as various other ethnic populations such as the German, Chinese, Swedish, Japanese, Bulgarian and Australian (Schwab *et*

al., 2003; Tang *et al.*, 2003; Van Den Bogaert *et al.*, 2003; Tochigi *et al.*, 2006; Kirov *et al.*, 2004; Holliday *et al.*, 2006). Although, there are still debates about the true nature of the association between dysbindin-1 and scz (Morris *et al.*, 2003; Joo *et al.*, 2006; Mutsuddi *et al.*, 2006; Peters *et al.*, 2008), dysbindin-1 represents one of the most promising risk factor for the disorder.

Analyses of post-mortem brains from patients diagnosed with scz have demonstrated reduction in dysbindin-1 protein and mRNA expression in certain brain structures (Talbot *et al.*, 2004; Weickert *et al.*, 2004), notably in intrinsic glutamatergic terminals of the hippocampus (Talbot *et al.*, 2004). The findings suggest a probable role of dysbindin-1 in the glutamatergic system. In accordance with this possibility, one study has provided evidence from cultured neurons that reduction in dysbindin-1 can lower basal and stimulus-induced glutamate release whereas over-expression elevates glutamate release (Numakawa *et al.*, 2004). Hypofunction in the glutamatergic system of several corticolimbic brain regions is currently proposed as a mechanism for the pathophysiology of scz: this hypothesis is founded on important observations that antagonist of the glutamatergic ionotropic receptor N-methyl-D-aspartate receptor (NMDAR), such as ketamine and phencyclidine, can produce psychotic and cognitive symptoms similar to those observed in scz (Javitt, 2007; Krystal *et al.*, 1994). Several postmortem studies have also confirmed region-specific changes in NMDAR and other glutamate markers in schizophrenic brains, such as reduction in NMDAR1 subtype expression in cortical region; a subtype that plays a key role in synaptic plasticity, synaptogenesis, excitotoxicity, memory acquisition and learning (Meador-Woodruff and Healy, 2000). Interestingly, certain pharmaceutical compounds, such as glycine or D-cycloserine, that are known to potentiate NMDAR neurotransmission, can considerably reduce the

cognitive and negative symptoms in scz subjects (Leiderman *et al.*, 1996; Yurgelun-Todd *et al.*, 2005), hereby further supporting the contribution of a hypoglutamatergic state to the scz phenotypes.

Neuropathological studies with autopsied brains from individuals with scz have reported many morphometrical changes and aberrations in neuronal cytoarchitecture. These structures again highlighted consistent changes in the PFC and hippocampus. Imaging investigations consistently demonstrated ventricular enlargement (Kelsoe, Jr. *et al.*, 1988; Shenton *et al.*, 2001), a feature that was found, from longitudinal studies, to progress slowly during course of the illness where its progression is associated with negative symptoms and poor function (Lieberman *et al.*, 2001; Whitworth *et al.*, 2005; d'Amato *et al.*, 1992). Widespread reduction of cortical thickness, mainly in prefronto-temporal regions (Kuperberg *et al.*, 2003; Nesvag *et al.*, 2008; Narayan *et al.*, 2007), have also consistently been observed. Hippocampal volume reduction in scz patients has also been shown in a number of studies (Nelson *et al.*, 1998; Heckers, 2001). Decreased levels of N-acetyl-aspartate were suggested to point towards a cellular basis of such volume changes (Heckers, 2001). Interestingly, both ventricular enlargement and cortical thinning were also observed in unaffected siblings of patients with scz (Goldman *et al.*, 2009; McDonald *et al.*, 2006; Silverman *et al.*, 1998; Lui *et al.*, 2009), thus indicating a possible association between these morphometric changes and the genetic liability for developing scz. In addition, ventricular enlargement (Lieberman *et al.*, 2001; Fannon *et al.*, 2000a; Fannon *et al.*, 2000b), reduction in cortical thickness (Venkatasubramanian *et al.*, 2008; Narr *et al.*, 2005b; Narr *et al.*, 2005a; Schultz *et al.*, 2010) and loss of hippocampal volume (Sumich *et al.*, 2002; Velakoulis *et al.*, 1999) were as well detectable in drug-naïve first episode psychosis patients. The later eliminate medication induced changes and

suggest disturbance of neurodevelopmental etiopathology at the onset of the disorder. A neurodevelopmental etiopathology differs from the more commonly disorder-associated neurodegenerative process where in the former early neurodevelopmental disturbances could interrupt the normal process of brain development and trigger cognitive and behavioral impairments during adolescent or early adulthood (Weinberger, 1995) .

Correlated with gross anatomical findings, post mortem neuropathological studies demonstrated several region specific cellular and cytoarchitectural changes in scz brains. Smaller neuron size, a measure correlated with a neuron's dendritic and axonal architecture, and lower neuronal density was detected in various cortical sub-regions that might be relevant to cortical thinning (Benes *et al.*, 1986; Benes and Bird, 1987; Pennington *et al.*, 2008). These results are, however, inconsistent as no change in neuronal counting (Stark *et al.*, 2004) and even higher neuronal density (Selemon *et al.*, 2003; Selemon *et al.*, 1995) were also reported in studies. Dr. David Lewis has provided, over the last decade, from a combination of analysis of Nissl-stained or immunoreactive sections, a thorough and profound investigation of the differences in pyramidal neuron, principal source of cortical glutamate neurotransmission, morphology in scz patients. In addition of the aforementioned cytoarchitectural changes, his group reported a reduced density of dendritic spines, the location of most excitatory inputs to pyramidal neurons, on dorsolateral prefrontal cortex pyramidal neurons in deep layer 3 of subjects with scz (Glantz and Lewis, 2000). More interestingly, the changes are lamina-specific (i.e. deep layer III reduction only and not layer 5 and 6 of the same subject; Kolluri *et al.*, 2005). Similar changes (i.e. reduction in pyramidal cell somal volume (Sweet *et al.*, 2003) and reduction in dendritic spine density (Sweet *et al.*, 2009)) were also reported in pyramidal

neurons located in deep layer 3 of auditory association cortex, hereby suggesting a common vulnerability of cortical glutamatergic neurons in schizophrenia.

Most of the functional research on dysbindin-1 is made available from studies on the *sd*y mouse animal model carrying an ablation of dysbindin-1A and -1C protein expression. This mouse model represents an excellent model to investigate brain functions of dysbindin-1 in vivo (Li *et al.*, 2003) and its involvement in *scz*. Decrease in dysbindin-1 in *sd*y mice was reported to impair membrane trafficking of NR2A receptors (Tang *et al.*, 2009). Further alterations of hippocampal neurophysiological properties were observed in the *sd*y model, including decrease frequency of spontaneous excitatory postsynaptic current (EPSC), smaller amplitude of evoked EPSC on CA1 pyramidal cells (Chen *et al.*, 2008) and impaired CA1 long-term potentiation (LTP; Jentsch *et al.* 2009) as compared to wild-type mice.

The validity of rodent animal models of disorders is often supported by their behavioural phenotypes. Over the years, behavioural neuroscientists have proposed a battery of behavioural, cognitive and psychopharmacological approaches designed to model the human neuropsychiatric conditions in the rodents (van der Staay *et al.*, 2009). These paradigms provide valuable information on phenotypic characterization of psychosis-related abnormalities in an animal model and give an important insight about the potential changes in the brain structure and neurotransmitter systems regulating a given behavioral/cognitive trait. A number of *scz*-relevant behavioral changes have been described in *sd*y mice. These include spatial and working memory deficits (Cox *et al.*, 2009; Takao *et al.*, 2008; Jentsch *et al.*, 2009), object recognition memory deficit (Bhardwaj *et al.*, 2008; Feng *et al.*, 2008), conditioned fear memory (Bhardwaj *et al.*, 2008), and deficits in social interaction (Feng *et al.*, 2008; Hattori *et al.*, 2008). While

there are disagreements among studies with respect to locomotor activity and anxiety, perhaps due to the use of mutants on different genetic backgrounds (e.g., DBA2/J vs. C57BL6J), a consistent finding is that dysbindin-1 mutants have deficits in cognitive functions some of which are dependent on the integrity of hippocampal networks. These cognitive abnormalities in *sd*y mice correlate with the reported association between genetic variations in dysbindin-1 and spatial working memory performance (Donohoe *et al.*, 2007), intellectual decline (Burdick *et al.*, 2007) and detrimental effect on general cognitive abilities (Burdick *et al.*, 2006) in the schizophrenic population. These behavioural abnormalities suggest aberration in the implicated brain region/neurotransmitter system, i.e. hippocampal glutamatergic system. Although the onset of *scz* is known to occur in adolescence/early adulthood, all reported behavioural phenotypes have only been studied in adulthood.

In light of the recent evidence, I aimed to investigate in my Masters project early differences in hippocampal glutamatergic transmission mediated by dysbindin-1 mutation using pre-pubertal offspring of Sandy mouse model and whether observed changes in early development would translate to adult morphological changes in hippocampal CA1 region. Our observations are restricted to the hippocampus: in addition to the neuropathological evidences highlighted earlier, functional neuroimaging studies have demonstrated abnormal levels of hippocampal activity at rest, during the experience of auditory hallucinations, and during the performance of memory retrieval tasks (Heckers, 2001). As such, the hippocampus is critical in the neuropathology and pathophysiology of *scz*.

2. Experimental design and approach

2.1 The Sandy mutant mice model

The *sd*y (*sd*y/+ and *sd*y/*sd*y) mutants arose from a spontaneous mutation on chromosome 13 that arose in the DBA/2J strain in 1983 and was maintained as a closed breeding colony using obligate *sd*y/+ mice. This mutation creates a natural 38-kb in-frame deletion in DTNBP-1, loss of amino acids 119-172 and the abolishment of dysbindin-1 protein expression (figure 1A), including that in the brain (Swank *et al.*, 1991), following degradation of truncated protein unable to bind to BLOC-1 complex. This deletion is not found in other mouse strains, including co-isogenic DBA/2J, indicating that it is not a strain-specific polymorphism. As assessed by daily observations, the gross appearance, body weight and cage activity of both genotypes of *sd*y mice appear normal to age-matched DBA/2J controls (*data not shown*). Brain surface appearance and weight of *sd*y mutants also appeared normal to age-matched controls (figure 1C).

The Jackson Laboratory (Bar Harbor, ME, USA) later backcrossed the homozygote *sd*y mice on the original DBA/2J background with pure C57BL.6J mice for 5 generations that were then intercrossed to obtain homozygous and heterozygous *sd*y mutants, on a C57/BL6 background (*sd*y/BL6 mice). These *sd*y/BL6 mice were transferred to their internal principal investigator Dr. L.L. Peters' laboratory and generously donated to Dr. L.K. Srivastava's laboratory at the Douglas Mental Health Institute. No significant difference in gross appearance, body weight, cage activity, and brain surface appearance and weight have been found between of both genotypes of these *sd*y/BL6 mice to age-matched C57/BL6 (*data not shown*).

2.2 Animal breeding

An in-house breeding program to generate homozygous and heterozygous *sd*y and wild-type controls is in place. Breeding is maintained by mating *sd*y/+ female and males in Plexiglas small shoe-box cages with Beta-chip bedding for seven to nine generations

after which mutants will be backcrossed with the co-isogenic inbred control strain to minimize genetic drift. At any time, we had a minimum of 5 breeding cages running to produce sufficient number of animals of each genotype. The genotype of the mice was identified by phenotype (sdy/sdy have light-grey sandy coat color whereas sdy/+ and W/T are undistinguishable; Figure 1B) as well as by genomic polymerase chain reaction (PCR) as reported by Cox *et al.* (2009). In summary, the mice were genotyped using a PCR procedure designed to yield PCR products across the segment of *Dtnbp1* deleted in sdy mice as originally reported by Li *et al.* (2003). A 472 base pair PCR product is yielded from the wild-type gene using the following primer sequences: SE3R (5'-AGCTCCACCTGCTGAACATT-3') and SE3F (5'-TGAGCCATTAGGAGATAAGAGCA-3'). A 274 base pair PCR product is yielded from the sdy gene using the following primer sequences: SF (5'-TCCTTGCTTCGTTCTCTGCT-3') and SR (5'-CTTGCCAGCCTTCGTATTGT -3'). The 472 base pair product is detected in wild-type and sdy/+ mice whereas the 274 base pair product is selectively detected in sdy/+ and sdy/sdy mice (figure 1D).

After weaning (PD 21), male and female mice were housed separately with equal numbers (3 each) of sdy/sdy, sdy/+ and WT mice in cages with cardboard toys, same room and conditions. Food intake, weight gain and general health of the animals were monitored daily. Male animals, homozygous and wild-type, at PD 10-11, 16-25 and 56-60 (n= 8-10 per genotype) were used for experiments. All cages were placed in a temperature/humidity controlled colony room, at approximately 21°C, maintained on a 12:12hr light/dark cycle (lights off at 8:00pm) with food and water available ad lib.

The procedures have been approved by the Animal Care Committee of the Douglas Mental Health Institute and McGill University, and were carried out in

accordance with the guidelines of the Canadian Council of Animal Care. Efforts were taken to minimize the number of animals used and their suffering during the experiments.

2.3 Fluorescent immunohistochemistry

PD 10-11, PD 21-25 DBA/2J (W/T), sdy/+ and sdy/sdy mice were sacrificed by decapitation and the brains removed rapidly and placed in ice-cold “low-CaCl₂” artificial cerebrospinal fluid (aCSF), pH 7.4, equilibrated with 95% O₂/5% CO₂, containing (in mM): 126 NaCl, 24 NaHCO₃, 10 glucose, 3 KCl, 2 MgSO₄, 1.25 NaH₂PO₄, and 1.2 CaCl₂, post-fixed by immersion in fresh 4% paraformaldehyde (diluted from 16% paraformaldehyde in a 2:1 solution of Phosphate Buffer (0.2mM/H₂O; PB); Sigma) overnight (o/n) at 4°C, transferred to sucrose 15% o/n and finally sucrose 30% o/n. All o/n incubations are at 4°C unless otherwise mentioned. Brains were embedded in a polymer solution (O.C.T. compound, Tissue Tek), quickly frozen in dry ice (CO₂) and sliced into sequential coronal sections of 20µm (60µm distance between slices) at the level of the dorsal hippocampus using a Cryostat LFICA CM 3050S.

Prior to protocol, the sections were rinsed 3 times in PB (0.1mM) for 15 minutes. The sections were transferred in a mixture of PB 0,1M /Triton 0,3% at 4°C for 30 minutes; followed by a blocking serum (3% NDS /2% BSA/ 0.1% Triton X-100 PBS); incubated o/n in a solution (PBS / 0.05% Triton X-100 PBS / 0.5% BSA) with primary antibodies against vesicular glutamate transporter 1/2 (vGLUT 1/2), synaptophysin (SYP), syntaxin-1A (SYN). As a positive control for vesicular changes, we assessed changes in main inhibitory neurotransmitter GABA, a system also heavily dysfunctional in scz (Li *et al.*, 2003), by quantifying expression of vesicular GABA transporter (vGAT). The concentrations are as follow: vGLUT1: 1:4000 (Millipore Chemicon); vGLUT2: 1:2000 (Synaptic System); vGAT: 1:1000 (Sigma Aldrich); synaptophysin: 1:400 (Santa

Cruz Biotechnology); syntaxin-1: 1:150 (Sigma Aldrich). The following day, the sections were rinsed 5 times in PB (0.1mM) during lapses of 5 minutes and transferred to a solution (PBS/ 0.05% Triton 10% / 0.5% BSA) with secondary antibody (Alexa 488 anti-rabbit: 1:500 or CY3 anti- guinea pig: 1:500 (both made in goat, Jackson ImmunoResearch)) for 2 hrs, completely covered by aluminum foiled to prevent light exposure. The reaction was stopped by rinsing the slices, again with minimum light exposure, as described above. Sections were mounted onto 3"X1" gel coated slides (LabScientifics Inc), with 1.0 µl DAPI-Vectashield (1:5; Vector Laboratories, Burlingame, CA, USA) to label nuclei, coverslipped with 50X24mm microscope cover glass (Fisher Scientific) and transparent nail polish. Adjacent to all immunostaining experiments, tissue from the same animal was processed at the same time in a separate well, all step identical but no primary antibody was used. This step was used to control for background level of the secondary antibody.

2.4 Modified Golgi-Cox staining

Brains were processed in modified Golgi-Cox staining solution as previously reported (Baharnoori *et al.*, 2008; Gibb and Kolb 1998). Briefly, brains were immersed in approximately 10ml of Golgi-Cox solution and stored in the dark for 21 days following which the solution was replaced with 30% sucrose for 5 consecutive days. Brains were sectioned with vibratome (VT1000S, Leica) at 150µm thickness in coronal plane at the level of hippocampus. The sections were placed on microslides (Snow-coat extra, Surgipath) and the blotted slides kept in humid chamber overnight. The section were later developed in ammonium hydroxide for 30 minutes and placed in Kodak film fixer for an additional 30 minutes. Sections were washed with water, dehydrated in graded ethanol (70%, 95%, 100%) and mounted using Permount (Fisher, SP15-100). Hippocampal CA1

pyramidal neurons were readily identified by their triangular shape of the soma and their apical extensions toward pial surface and numerous dendritic spines. The criteria used to select neurons for reconstruction were essentially as was described previously (Baharnoori *et al.*, 2009). In short, (1) only neurons that with apical and basilar dendritic trees that were fully impregnated with Golgi solution were traced; (2) only neurons which were not covered by the dendritic tree of the other neurons in their vicinity were selected; and (3) only neurons that had the dendrites with third branch order or more were traced hereby omitting very small neurons.

2.5 Data analysis

A subregional relative quantification of the immunolabeling in the CA1, CA3 (str. alveus-oriens, str. pyramidale, str. radiatum and str. lacunosum-moleculare) and DG (granular cell layer, molecular layer, hilus and polymorphic layer) was performed using Image J (NIH). Fluorescence intensity was measured over a representative region ($150\mu\text{m} \times 30\mu\text{m}$, $4500\mu\text{m}^2$) on sections analyzed using a camera-enable microscope (Nikon Instruments) at 20X magnification as described in Chao *et al.*, (2008). Analysis was performed on an average of five sections per mouse. Obtained fluorescent intensity values from tissues stained with primary antibody were subtracted from tissues-stained without primary antibody to remove background non-specific fluorescent emission from secondary antibody. To control for experimenter biases, the slides were coded and the pictures randomized. All results are expressed as mean \pm SD. Data from mean subregional fluorescent intensity acrossed genotypes were analyzed using two-way ANOVA with genotypes and subregions as independent variables. Post-hoc Bonferroni analysis was applied whenever appropriate.

For Golgi-Cox staining, soma and apical/basilar dendritic segments were traced and reconstructed three-dimensionally using a Leica microscope (Leica DM5000B; 20X magnification) together with a motor stage equipped with transducers on the XYZ-axes (NEUROLUCIDA, MicroBrightField system, Williston, VT). For each animal; 5 sections/ per region and in each section, one neuron/ hemisphere were selected for analysis. The number of dendritic branching was assessed by Sholl analysis by counting the number of intersections on an overlay of concentric rings (10 μm interval between rings, as shown in figure 7b). The total length of dendrites was also calculated by Sholl analysis using NeuroLucida system. For spine density measurements, one terminal dendrite from the third order tip (minimum length 20 μm) of each selected neuron was used to count spines at a magnification of 100X. The results are expressed as number of spines/10 μm . We only traced the spines that were fully attached to dendritic segments and avoided the spines whose structure was not completely visible in the microscope. For each selected dendrite, spine density and spine structure was evaluated as spine length (μm) surface area (μm^2) and volume (μm^3) according to NeuroLucida software. All statistical analyses were performed using Prism version 4.0 (GraphPad Software, Inc., San Diego, CA, USA). *N* represents number of mice. Data from mean soma size, dendritic arborization, total dendritic length, spine density, spine length, spine surface and spine volume acrossed genotypes were analyzed using ANOVA.

3. Results

3.1. Fluorescent immunohistochemistry

3.1.1 Fluorescence intensity of vesicular-glutamate-transporter-1 protein expression

3.1.1.1 CA1

Two-way ANOVA at P10-11 demonstrated significant main effect of genotype $F(2, 24= 8.860, P= 0.0013)$, but no interaction between subregions and genotype $F(6, 24= 0.2758, P= 0.9428)$. Post-doc analyses indicated a significant decrease in fluorescent intensity in homozygous *sdv/sdv* mutants as compared to control DBA/2J, in lacunosum-moleculare (*lac/mol*, $P < 0.05$). The results are shown in Figure 2 a-b. ANOVA at P 21-25 demonstrated a significant main effect of genotype $F(2, 48= 22.33, P<0.0001)$ but no interaction $F(6, 48= 0.2950, p= 0.9364)$. Post-doc analyses indicated a significant difference between DBA/2J and *sdv/sdv* in most subregions of the CA1 (*alveus/oriens* (*alv/ori*), $P < 0.05$; *radiatum* (*rad*), $P<0.01$; *lac/mol*, $P<0.01$). The results are shown in Figure 2 c-d.

3.1.1.2 CA3

Two-way ANOVA at P10-11 demonstrated a significant main effect of genotype $F(2, 30= 7.641, P= 0.0021)$ but no interaction $F(8, 30= 0.2486, P= 0.9774)$. The results are shown in Figure 2 a-b. ANOVA at P21-25 demonstrated a significant main effect of genotype $F(2, 48= 73.49, P<0.0001)$ but no interaction $F(6, 48= 1.020, p= 0.4310)$. Post-doc analysis indicated a significant decrease in fluorescent intensity in homozygous *sdv/sdv* mutants as compared to control DBA/2J at all subregions of the CA3 (*alv/ori*, $P<0.001$; *pyramidal layer* (*pyr*), $P<0.001$; *lucidum* (*luc*), $P<0.001$; *rad*, $P<0.001$; *lac/mol*, $P<0.05$). The results are shown in Figure 2 c-d.

3.1.1.2 DG

Two-way ANOVA at P10-11 demonstrated a significant main effect of genotype $F(2, 24= 6.015, P= 0.0076)$ but no interaction between subregions and genotype $F(6, 24= 0.9651, P= 0.4693)$. Post-doc analyses indicated a significant decrease in fluorescent intensity in homozygous *sdv/sdv* mutants as compared to control DBA/2J in molecular

layer (mol. layer, $P < 0.05$). The results are shown in Figure 2 a-b. ANOVA at P21-25 demonstrated a significant main effect of genotype $F(2, 48 = 39.27, P < 0.0001)$ but no interaction $F(6, 48 = 0.4483, p = 0.8426)$. Post-doc analysis test indicated a significant decrease in fluorescent intensity in homozygous *sdv/sdv* mutants as compared to control DBA/2J at all subregions of the DG (granular layer (gran), $P < 0.01$; mol. layer, $P < 0.01$; hilus, $P < 0.001$; polymorphic layer (pol. layer), $P < 0.001$). The results are shown in Figure 2 c-d.

3.1.2 Fluorescence intensity of vesicular-glutamate-transporter-2 protein expression

3.1.2.1 CA1

Two-way ANOVA of CA1 at P10-11 demonstrated a significant main effect of genotype $F(2, 24 = 85.18, P < 0.0001)$ but no interaction $F(6, 24 = 1.580, P = 0.1960)$. Post-doc revealed significant decrease in fluorescent intensity in homozygous *sdv/sdv* mutants as compared to control DBA/2J (alv/ori, $P < 0.001$; pyr, $P < 0.001$; rad, $P < 0.001$; lac/mol $P < 0.001$) and between DBA/2J and *sdv/+* (alv/ori, $P < 0.05$; pyr, $P < 0.001$; rad, $P < 0.01$; lac/mol, $P < 0.001$). The results are shown in Figure 3a-b. ANOVA at P21-25 demonstrated no significant main effect of genotype $F(2, 24 = 0.1717, P = 0.8432)$ nor interaction between subregions and genotype $F(6, 24 = 0.5093, P = 0.7952)$. The results are shown in Figure 3c-d.

3.1.2.2 CA3

Two-way ANOVA of CA3 at P10-11 demonstrated a significant main effect of genotype $F(3, 24 = 99.03, P < 0.0001)$ but no interaction $F(6, 24 = 0.4693, P = 0.8242)$. Post-doc revealed a significant decrease in fluorescent intensity in homozygous *sdv/sdv* mutants as compared to control DBA/2J in all subregions of CA3 (alv/ori, $P < 0.001$; pyr, $P < 0.001$; rad, $P < 0.001$; lac/mol $P < 0.001$) as well as between DBA/2J and *sdv/+* (alv/ori, $P < 0.001$;

pyr, $P < 0.001$; rad, $P < 0.001$; lac/mol, $P < 0.01$). The results are shown in Figure 3a-b. ANOVA at P21-25 demonstrated no significant main effect of genotype $F(2, 24 = 2.594, P = 0.0955)$ nor interaction $F(6, 24 = 0.8493, P = 0.5451)$. The results are shown in Figure 3c-d.

3.1.2.3 DG

Two-way ANOVA of DG at P10-11 demonstrated a significant main effect of genotype $F(2, 24 = 106.3, P < 0.0001)$ and no interaction $F(6, 24 = 0.2424, P = 0.9577)$. Post-doc revealed a significant decrease in fluorescent intensity in homozygous *sdv/sdv* mutants as compared to control DBA/2J in all subregions of DG (gran, $P < 0.001$; mol. layer, $P < 0.001$; hilus, $P < 0.001$; pol. layer, $P < 0.001$) as well as between DBA/2J and *sdv/+* (gran, $P < 0.001$; mol. layer, $P < 0.001$; hilus, $P < 0.001$; pol. layer, $P < 0.001$). The results are shown in Figure 3a-b. ANOVA at P21-25 demonstrated no significant main effect of genotype $F(2, 24 = 0.3430, P = 0.7130)$ nor interaction $F(6, 24 = 0.3229, P = 0.9185)$. The results are shown in Figure 3c-d.

3.1.3 Fluorescence intensity of synaptophysin protein expression

3.1.3.1 CA1

Two-way ANOVA at P10-11 demonstrated no significant main effect of genotype $F(2, 24 = 1.794, P = 0.1878)$ nor interaction between subregions and genotype $F(6, 24 = 0.04476, P = 0.9995)$. The results are shown in Figure 4a-b. ANOVA at P 21-25 demonstrated a significant main effect of genotype $F(2, 48 = 38.91, P < 0.0001)$ but no interaction $F(6, 48 = 0.2484, p = 0.9576)$. Post-doc analyses indicated a significant decrease in fluorescent intensity in homozygous *sdv/sdv* mutants as compared to control DBA/2J in all subregions of the CA1 (alv/ori, $P < 0.01$; pyr, $P < 0.001$; rad, $P < 0.001$; lac/mol, $P < 0.01$). The results are shown in Figure 4c-d.

3.1.3.2 CA3

Two-way ANOVA at P10-11 demonstrated no significant main effect of genotype $F(2, 30 = 1.988, P = 0.1546)$ nor interaction $F(8, 30 = 0.1782, P = 0.9922)$. The results are shown in Figure 4a-b. ANOVA at P21-25 demonstrated a significant main effect of genotype $F(2, 50 = 23.22, P < 0.0001)$ but no interaction $F(16, 50 = 0.2434, p = 0.9984)$. Post-doc analysis indicated a significant decrease in fluorescent intensity in homozygous *sdv/sdv* mutants as compared to control DBA/2J at all subregions of the CA3 (*alv/ori*, $P < 0.001$; *pyr*, $P < 0.001$; *luc*, $P < 0.001$; *rad*, $P < 0.001$; *lac/mol*, $P < 0.05$). The results are shown in Figure 4c-d.

3.1.3.3 DG

Two-way ANOVA at P10-11 demonstrated no significant main effect of genotype $F(2, 24 = 1.165, P = 0.3289)$ nor interaction between subregions and genotype $F(6, 24 = 0.2472, P = 0.9557)$. The results are shown in Figure 4a-b. ANOVA at P21-25 demonstrated a significant main effect of genotype $F(2, 48 = 39.92, P < 0.0001)$ but no interaction $F(6, 48 = 0.4888, p = 0.8135)$. Post-doc analysis test indicated a significant decrease in fluorescent intensity in homozygous *sdv/sdv* mutants as compared to control DBA/2J at all subregions of the DG (*gran*, $P < 0.01$; *mol. layer*, $P < 0.01$; *hilus*, $P < 0.001$; *pol. layer*, $P < 0.001$). The results are shown in Figure 4c-d.

3.1.4 Fluorescence intensity of syntaxin-1 protein expression

3.1.4.1 CA1

Two-way ANOVA of CA1 at P10-11 demonstrated no significant main effect of genotype $F(2, 24 = 1.794, P = 0.1878)$ nor interaction $F(6, 24 = 0.04476, P = 0.9995)$. The results are shown in Figure 5a-b. ANOVA at P21-25 demonstrated no main effect of

genotype $F(2, 46= 0.3336, P=0.7185)$ nor interaction $F(6, 36= 0.1165, p= 0.9938)$. The results are shown in Figure 5c-d.

3.1.4.2 CA3

Two-way ANOVA of CA3 at P10-11 no significant main effect of genotype $F(2, 30= 1.988, P= 0.1546)$ nor interaction between subregions and genotype $F(8, 30= 0.1782, P= 0.9922)$. The results are shown in Figure 5a-b. ANOVA at P21-25 demonstrated no significant main effect of genotype $F(2, 36= 0.9548, P=0.3944)$ nor interaction $F(6, 36=0.1719, P=0.9827)$. The results are shown in Figure 5c-d.

3.1.4.3 DG

Two-way ANOVA of DG at P10-11 demonstrated no significant main effect of genotype $F(2, 24= 1.165, P= 0.3289)$ nor interaction $F(6, 24= 0.2472, P= 0.9557)$. The results are shown in Figure 5a-b. ANOVA at P21-25 demonstrated no significant main effect of genotype $F(2, 24= 1.002, P= 0.4090)$ nor interaction $F(6, 24= 0.2137, p= 0.9688)$. The results are shown in Figure 5c-d.

3.1.5 Fluorescence intensity of vesicular-GABA-transporter protein expression

3.1.5.1 CA1

Two-way ANOVA of CA1 at P10-11 demonstrated a significant main effect of subregions $F(3, 24= 6.419, P= 0.0024)$, no significant main effect of genotype $F(2, 24= 1.526, P=0.2378)$ and no interaction $F(6, 24= 0.09494, P= 0.9963)$. The results are shown in Figure 6a. Two-way ANOVA at P21-25 demonstrated a significant main effect of genotype $F(2, 24= 3.776, P= 0.0375)$, a significant main effect of subregions $F(2, 24= 13.97, P<0.0001)$ but no interaction between subregions and genotype $F(6, 24= 0.9991, P= 0.4486)$. The results are shown in Figure 6b.

3.1.5.2 CA3

Two-way ANOVA of CA3 at P10-11 demonstrated a significant main effect of genotype $F(2, 30= 5.276, P= 0.0109)$, a significant main effect of subregions $F(4, 30= 11.46, P<0.0001)$ but no interaction $F(8, 30= 0.2977, P= 0.9611)$. The results are shown in Figure 6a. Two-way ANOVA at P21-25 demonstrated a significant main effect of genotype $F(2, 30= 8.958, P= 0.0009)$, a significant main effect of subregions $F(4, 30= 4.228, P= 0.0078)$ but no interaction between subregions and genotype $F(8, 30= 0.6383, P= 0.7393)$. The results are shown in Figure 6b.

3.1.5.3 DG

Two-way ANOVA of DG at P10-11 demonstrated a significant main effect of genotype $F(2, 24= 0.5092, P= 0.6073)$, a significant main effect of subregions $F(3, 24= 5.110, P= 0.0071)$ but no interaction between subregions and genotype $F(6, 24= 0.1439, P= 0.9886)$. The results are shown in Figure 6a. Two-way ANOVA at P21-25 demonstrated a significant main effect of genotype $F(2, 24= 4.009, P= 0.0315)$, a significant main effect of subregions $F(3, 24= 42.84, P<0.0001)$ but no interaction between subregions and genotype $F(6, 24= 1.085, P= 0.3993)$. The results are shown in Figure 6b.

3.2 CA1 neuronal morphology: Modified Golgi-Cox staining

Figure 7a shows representative photomicrographs of Golgi stained CA1 sections in control DBA/2J mice at P60.

3.2.1 Soma size

Student's two-tailed t-test demonstrated a significant increase in soma size in sdy/sdy as compared to control DBA/2J ($P= 0.0066$). The results are shown in Figure 7c.

3.2.2 Dendritic arborization

Two-way ANOVA of the number of apical dendritic intersections displayed a significant main effect of genotype on dendrite arborization pattern ($F_{(1, 414)} = 74.44$, $P < 0.0001$), significant main effect of radius ($F_{(45, 414)} = 96.35$, $P < 0.0001$), but no significant interaction between treatment x radius ($F_{(45, 414)} = 1.246$, $P < 0.0001$). Bonferroni post-hoc analysis revealed an increased branching of apical dendrites in *sd*/*sd* as compared to DBA/2J at radius 290 μm ($P < 0.05$) and 300 μm ($P < 0.01$) as compared to DBA/2J at same radius. The results are shown in Figure 8a. Two-way ANOVA of the Sholl analysis of the number of basilar dendritic intersections displayed no significant main effect of genotype on dendrite arborization pattern ($F_{(1, 252)} = 1.959$, $P = 0.1629$), a significant main effect of radius ($F_{(27, 252)} = 145.9$, $P < 0.0001$), but no significant interaction between treatment x radius ($F_{(27, 252)} = 0.2036$, $P = 1.0000$). The results are shown in Figure 8b.

3.2.3 Total dendritic length

Student's two-tailed t-test of total apical dendritic length displayed significant increase in *sd*/*sd* as compared to DBA/2J ($P = 0.0441$). Tukey Post-doc analyses indicated a significant increase in *sd*/*+* as compared to DBA/2J ($p < 0.05$). The results are shown in Figure 9a. Student's two-tailed t-test of total basilar dendritic length displayed no significant differences between genotypes ($P = 0.8575$). The results are shown in Figure 9b.

3.2.4 Spine density

Student's two-tailed t-test of apical spine density displayed a significant increase in *sd*/*sd* as compared to DBA/2J ($P = 0.0204$). The results are shown in Figure 10a. Student's two-tailed t-test of basilar spine density displayed not significant difference in

between genotypes ($P=0.6402$). Tukey post-doc analyses indicated a significant increase in sdv/sdy as compared to DBA/2J ($P < 0.01$). The results are shown in Figure 10b.

3.2.5 Spine length

Student's two-tailed t-test of apical spine length displayed no significant difference between genotypes ($P= 0.5774$). The results are shown in Figure 11a. Student's two-tailed t-test of basilar spine length displayed a significant decrease sdv/sdy as compared to DBA/2J ($P= 0.0166$). The results are shown in Figure 11b.

3.2.6 Spine surface

Student's two-tailed t-test of apical spine surface displayed no significant difference between genotypes ($P= 0.7291$). The results are shown in Figure 12a. Student's two-tailed t-test of basilar spine surface displayed a significant decrease in sdv/sdy as compared to DBA/2J ($P= 0.0107$). The results are shown in Figure 12b.

3.2.7 Spine volume

Student's two-tailed t-test of apical spine volume displayed no significant difference between genotypes ($P= 0.7585$). The results are shown in Figure 13a. Student's two-tailed t-test of basilar spine volume displayed a significant decrease in sdv/sdy as compared to DBA/2J ($P= 0.0066$). The results are shown in Figure 13b.

4.0 Discussion

4.1 Discussion of pre-synaptic vesicular changes

The present study provides evidence supporting the role of dysbindin-1 in glutamatergic synapses and demonstrates the involvement of dysbindin-1 in the destabilization of glutamate vesicular phenotype. Glutamate has been accepted as the most abundant excitatory neurotransmitter in the adult central nervous system (Fonnum, 1984), and glutamatergic neurons and glutamate-mediated excitatory signaling are

implicated in all neuronal circuits of the central nervous system (Moriyama and Yamamoto, 2004). The discovery that three members of the solute carrier family, Slc17a6–8, act as vesicular glutamate transporters (hence named vGLUT1, 2, 3) has enabled proper identification of glutamate signaling neurons and studies of glutamatergic neurotransmission (Bellocchio *et al.*, 2000; Fremeau *et al.*, 2001; Takamori *et al.*, 2000): as such, VGLUT1 and vGLUT2 are pre-synaptic markers which are specifically located on the glutamatergic axon terminals, thus making them reliable markers for glutamatergic neurons. They control the excitatory neurotransmitter signal by re-uptake of released glutamate from the synaptic extracellular space (Danbolt, 2001). Interestingly, we observed decreases in vGLUT1 and vGLUT2 at different stages of postnatal development: where down-regulation of vGLUT2 was only shown in immediate early post-natal period (PD 10-11) but decreased in vGLUT1 was only observed in third post-natal week. These reductions coincide with their respective window of peak expression levels within the hippocampus (Fremeau *et al.*, 2004b). Indeed, there is a transient higher expression level of vGLUT2 in early postnatal period in the developing brain following which vGLUT2 expression declines toward adulthood. On the other hand, vGLUT1 expression increases during postnatal development, gradually replacing vGLUT2 in several regions including neocortex (Boulland *et al.*, 2004). Their expression appears to be spatially complementary. The spatial distribution is not absolute (e.g. vGLUT2 is expressed in subpopulations of the cerebral cortex and hippocampus throughout life; Wallen-Mackenzie *et al.*, 2010). Interestingly, aside from their mostly segregated local expression, vGLUTs are associated with functionally distinct synaptic sites. VGLUT1 is preferentially expressed in terminals with low release probability (e.g. parallel fibers), whereas VGLUT2 is restricted to the fibers with higher release probability such as

climbing fibers in cerebellum (Fremeau *et al.*, 2004a) It is believed that the differential synaptic regulation create a fine-tuning system for glutamatergic transmission according to the needs of that region and the specific developmental stage (Fremeau *et al.*, 2001; Fremeau *et al.*, 2004a).

Decrease in vGLUT1 mRNA (Harrison and Eastwood, 2003) and protein expression (Eastwood and Harrison, 2005) have previously been demonstrated in tissue from scz patients. My results are in support to the trend in the literature. As seen in rodents, vGLUT2 mRNA and protein expression are sparse in the adult human hippocampus (for review see Harrison *et al.*, 2003). Attempts have yet reliably quantified neither gene product (as referenced in Harrison and Eastwood, 2003; unpublished observations from Harrison *et al.*, 2003). No current reports in the literature support my novel finding of alteration in vGLUT2 expression.

We acknowledge that our current method of analysis does not allow us to count the actual number of vGLUT1/2 transporter on a single vesicle, hereby our relative quantification might either reflect a decrease in number of glutamatergic vesicles or a decrease of number of vGLUT1/2 per vesicle. However, based on the recent results from Chen *et al.* (2008), we can conclude that the observed decrease reflect changes in vesicle number. The reductions in SYP, a general marker of vesicles, support this conclusion.

All hippocampal subfields receive an abundance of intrinsic hippocampal tri-synaptic and extrinsic afferents, of which include glutamatergic inputs originating in the enthorhinal cortex (EC) and other ipsilateral and contralateral hippocampal subregions. Our preliminary analysis of EC from DBA/2J, *sdyl/+* and *sdyl/sdy* did not show decrease of vGLUT1/vGLUT2 fluorescent expression in regions receiving extrinsic projections

(*data not shown*), hereby suggesting a fundamental decrease in vGLUT1/vGLUT2 on axons of the intrinsic tri-synaptic pathway.

Synaptophysin, a 38-kd integral membrane protein of small synaptic vesicles (Südhof *et al.*, 1987; Navone *et al.*, 1986), appears to be critical for calcium dependent synaptic transmission (Alder *et al.*, 1992; Alder *et al.*, 1995). Synaptophysin is present in more than 95% of cortical synaptic terminals and levels of synaptophysin immunoreactivity have been shown to be reliable measures of synaptic density (Masliah *et al.*, 1990). Although no changes have been found at the protein level, synaptophysin messenger RNA was reduced bilaterally in regions of the hippocampal and parahippocampal formation (Eastwood *et al.*, 1995) of schizophrenic cases.

We quantitatively investigated the changes in SYP to assess the integrity of hippocampal synaptic circuitry in the sandy model. We observed a decrease in SYP expression in all subregions of CA1, CA3 and DG at PD21-25. Again, the observed decrease may translate to decrease in number of vesicles or number of SYP per vesicles. Eastwood *et al.* (1995) reported that their observed decreases in SYP mRNA were also associated with a decrease in terms of grains per pyramidal neuron in the affected subfields. We cannot readily conclude from our results for one or another.

Since synaptophysin is a general marker for synaptic vesicles, decrease in SYP suggests that other hippocampal neurotransmitters trafficking could be affected. As such, dysbindin-1 has been associated with the dopaminergic system whereby decrease in dysbindin-1 results in decrease in total, vesicular and cytosolic, dopamine level in the hippocampus (Murotani *et al.*, 2007). Pharmacological and neuropathological evidence suggests that dysfunction of dopaminergic, glutamatergic, or GABAergic transmission underlies the symptomatology of scz (Coyle, 2006). Since the expression of dysbindin-1

is found to be co-localized to vesicular fragment, we investigated the possible effect of dysbindin-1 on GABAergic transmission by measuring changes in the transporter of GABA (vesicular GABA transporter; vGAT). Dysbindin-1 does not appear to play a general role in all vesicular trafficking as no significant changes have been observed in vGAT. This data is further supported by evidence from Talbot *et al.* (2004) showing that the dysbindin-1 protein was not localized in known terminal fields of nonglutamatergic transmitter systems in the hippocampal formation (i.e., cholinergic, GABAergic, or monoaminergic systems). Similarly, due to our technical limitation, for reason previously advanced, we cannot explicitly advance that the GABAergic system is intact. Furthermore, no changes in the syntaxin-1, marker of presynaptic density was observed.

In conclusion, the reductions of dysbindin-1 expression reported in scz may contribute to the glutamate hypofunction by decreasing the number of glutamatergic synaptic vesicles while likely preserving presynaptic terminal density.

4.2 Discussion of morphology changes

This present study provides first evidence supporting the role of dysbindin-1 in cytoarchitecture of hippocampal CA1 pyramidal neurons. We observed increase in soma size and dendritic arborization and total dendritic length of apical dendrites. Interestingly, our results also showed predominant changes in spine morphology with decrease in spine length, surface and volume in conjunction to an increase in spine density in basilar dendrites. This particular cytoarchitectural phenotype has never previously been observed in models of scz but rather reminiscent of the mice fragile-X syndrome with deficiency in fragile-X mental retardation protein, the protein absent in those afflicted with fragile-X syndrome (Irwin *et al.*, 2000). The later changes were unanimously observed in basilar dendrites alone, hereby suggesting a region-specific regulatory mechanism.

Our observations indicate that decrease in dysbindin-1 protein expression may more particularly affect the mechanism that promote basilar spine formation, whereas mechanisms that regulate apical spine formation and apical/basilar dendrite elongation and branching may be altered in a complex manner interacting with subregional-specific mechanisms.

Interestingly, previous neuroanatomical studies have shown scz-associated changes in PFC (i.e. increase in neuron density in areas 9 and 10 (Benes *et al.*, 1991; Selemon *et al.*, 1995), decrease of neuronal somal size in the PFC (Rajkowska *et al.*, 1998), and specifically the somal size of pyramidal neurons of layer III (Pierri *et al.*, 2001), and lower density of dendritic spines (Garey *et al.*, 1998; Glantz and Lewis, 2000). Although PFC has generally been associated with the cognitive symptoms related to the disorder, a number of morphological abnormalities of the hippocampal formation are also reported for schizophrenic brains (i.e. reduction in hippocampal size in MRI studies, Proton magnetic resonance imaging shows a reduced N-acetyl aspartate signal, indicative of a neuronal pathology at all phases of the illness; positron emission tomography studies reveal symptom-related alterations in hippocampal metabolic activity; animal models showing the consequences of neonatal hippocampal damage in rodents and non-human primates (for review see Harrison 2004 Harrison 1995; Harrison 1999). Rosoklija *et al.* (2000) reported significantly lower spine density in schizophrenia and mood disorder groups as compared to nonpsychiatric control group in postmortem analysis of subiculum. In light of the close association between hippocampal and parahippocampal structure, the later suggest a potential spine-specific aberration in the hippocampal.

The observed neuronal morphological changes may result from post-synaptic developmental abnormalities. Dysbindin-1 interacts with a number of proteins involved in

regulating neuronal morphology. The BLOC-1 complex is involved in vesicle trafficking (Li *et al.*, 2003), neurite growth (Ghiani *et al.*, 2010) and dendritic branching (Chen *et al.* 2005). Abolition of BLOC-1 complex, of which dysbindin-1 is an integral member, has been demonstrated to result in significant neurite atrophy in cultured hippocampal neuron (Ghiani *et al.*, 2009). More specific to dysbindin-1, recent studies have isolated the precise involvement of the dysbindin-1 protein in the process: dysbindin-1 was found to be positively-associated with the phosphorylation levels of c-Jun N-terminal kinase (JNK), a kinase involved in the phosphorylation of many cytoskeletal proteins and regulation of neural development (Bjorkblom *et al.*, 2005; Gdalyahu *et al.* 2004). As such, RNA interference-mediated knockdown (siRNA-kd) of dysbindin-1 in SH-SY5Y cells dramatically disrupted organization of actin cytoskeleton at the tips of neurites (Kubota *et al.*, 2009) . This effect was also observed in cultured hippocampal cells from embryonic sdy mice (Kubota *et al.*, 2009). First evidence of dysbindin-1 role in spine morphogenesis was recently demonstrated by Ito *et al.* (2010): they demonstrated, from immunofluorescent analyses, that dysbindin-1 is enriched at spine-like structure in primary cultured rat hippocampal neurons and siRNA-kd of dysbindin-1 led to the generation of abnormally elongated immature dendritic protrusions. Dysbindin-1 also regulates actin polymerization by promoting the binding of WAVE-2 to Abi-1 (Ito *et al.*, 2010), an interaction essential for mediating the actin reorganization properties of the WAVE2 protein family (Innocenti *et al.* 2005). WAVE-2 and Abi-1 interaction has been shown to have essential functions in dendrite morphogenesis and synapse formation (Proepper *et al.*, 2007; Soderling *et al.*, 2007). The siRNA-kd of dysbindin-1 led to the generation of abnormally elongated immature dendritic protrusions in rat primary cultured hippocampal neurons (Ito *et al.*, 2010). Hereby, the observed pyramidal cell morphology

may result from the indirect influence of dysbindin-1 protein on cytoskeleton via phosphorylation of target actin polymerization proteins.

Although molecular evidences suggest underlying effects of dysbindin-1 on projection of cellular processes, the main significance of our findings lies in the subregional differences between apical and basilar dendritic arbor. Region specific differences in apical and basilar dendrites have been previously observed in post-mortem studies of PFC dendritic architecture of scz-diagnosed patients (Kalus *et al.*, 2000). In the hippocampus, in addition to having unique intrinsic properties, basilar and apical dendrites are targeted differently by Schaffer collaterals and entorhinal perforant path fibers, respectively, where afferents to basilar dendrites derive mainly from CA3 pyramidal cells far from the dentate hilus (i.e., CA3a) and afferents to apical dendrites derive mainly from CA3 pyramidal cells close to the hilus (i.e., CA3c). Growth of new spines and changes in the structure of existing spines are possible substrates of synaptic plasticity in the hippocampus (Grutzendler *et al.*, 2002; Trachtenberg *et al.*, 2002).

Long-term potentiation (LTP) of synaptic strength, a glutamate-dependent physiological mechanism, has been shown to influence the maintenance, shape and growth of dendritic spines through the membrane trafficking from recycling endosomes (Park *et al.*, 2006). As such, morphological state of the CA1 pyramidal neurons is directly correlated to the potentiation of synaptic transmission. A current-source density study of LTP of commissural afference to hippocampal CA1 has shown that the basilar dendrites are more excitable than the apical dendrites (Kaibara et Leung, 1993). The ability of CA3 to drive CA1 pyramidal cells would be weakened by the absence of dysbindin-1 in the sandy mice. This mechanism likely underlies disturbances in glutamatergic neurotransmission that have been frequently reported in sandy mutants and in scz that can

lead to alteration of dendritic spines with consequential major pathological changes in brain function. Our findings may thus reflect differential effects of dysbindin-1 loss on output of CA3a and CA3c. The increase in basilar dendrite spine density may hereby compensate for the decrease in pre-synaptic stimulation as no changes in presynaptic terminal density were observed in the homozygous mutant.

The synapse is one of the most promising sites of convergence in regard to molecular pathways for mental conditions. The observed changes in *sd*y may have important consequences, since hippocampal pyramidal neurons are engaged in the processing of cognitive functions (Kawabe and Miyamoto, 2008). On the other hand, an increasing number of studies have shown that cytoskeletal organization is essential for the dynamics of synaptogenesis (Pak *et al.*, 2008; Sekino *et al.*, 2007). In light of the peculiar synaptic distribution of dysbindin-1, the observed cytoarchitectural changes may be the net-output of both pre- and post-synaptic compensatory modulations in the *sd*y model rather than one or the other. The isoforms of dysbindin-1 are segregated at the synapse formation (dysbindin-1A, the predominant form, highly concentrated in PSD fractions, 1-B, the human-exclusive isoform, in pre-synaptic fractions and 1-C in both), and might then perform very different roles.

In conclusion, our results in sandy mice suggest that the reduction of dysbindin-1 expression reported in *scz* perhaps also contributes post-synaptically to altered hippocampal synaptic transmission through immaturity or atrophy of spines. Although the physiological implications of differentially altered apical and basilar dendrites and spines remains to be established, it can be postulated that this would likely result in differential alterations of the responsiveness to the input specific to each regions. These changes in

response to a reduction in dysbindin-1 could well contribute to the alteration in hippocampal function observed in Sandy mice and be an important marker in scz.

5. Acknowledgements

This research was supported by a grant from the Canadian Institute of Health Research to Lalit K. Srivastava and Sylvain Williams.

I would like to thank Dr. Marc Danik for assistance in the creation of the immunohistochemistry protocol, Dr. Moogeh Baharnoori for the Golgi-Cox procedure and neuron tracing analysis, Ivonne Lachapelle for assistance in the neuron tracing, Dr. Romain Goutagny and Jesse Jackson for assistance in analysis of theta oscillations.

I thank my advisory committee, Dr. Naguib Mechawar, Dr. Tak Pan Wong for their advice and supervisors Dr. Lalit K. Srivastava and Dr. Sylvain Williams for their supervision, advice and guidance.

6. References

- Alder J, Kanki H, Valtorta F, Greengard P, Poo MM. (1995). Overexpression of synaptophysin enhances neurotransmitter secretion at *Xenopus* neuromuscular synapses. *J Neurosci.*, 15(1 Pt 2): 511-9.
- Alder J, Lu B, Valtorta F, Greengard P, Poo MM. (1992). Calcium-dependent transmitter secretion reconstituted in *Xenopus* oocytes: requirement for synaptophysin. *Science*, 257(5070): 657-61.
- Axmacher N, Henseler MM, Jensen O, Weinreich I, Elger CE, Fell J. (2010). Cross-frequency coupling supports multi-item working memory in the human hippocampus. *Proc Natl Acad Sci U S A*, 107(7): 3228-33.
- Baharnoori M, Brake WG, Srivastava LK. (2009). Prenatal immune challenge induces developmental changes in the morphology of pyramidal neurons of the prefrontal cortex and hippocampus in rats. *Schizophr Res.*, 107(1): 99-109.
- Bellocchio EE, Reimer RJ, Fremeau RT Jr, Edwards RH. (2000). Uptake of glutamate into synaptic vesicles by an inorganic phosphate transporter. *Science*, 289: 957–60.
- Benes FM, Bird ED. (1987). An analysis of the arrangement of neurons in the cingulate cortex of schizophrenic patients. *Arch Gen Psychiatry*, 44: 608-616.
- Benes FM, Davidson J, Bird ED. (1986). Quantitative cytoarchitectural studies of the cerebral cortex of schizophrenics. *Arch Gen Psychiatry*, 43: 31-35.
- Benes FM, McSparren J, Bird ED, SanGiovanni JP, Vincent SL. (1991). Deficits in small interneurons in prefrontal and cingulate cortices of schizophrenic and schizoaffective patients. *Arch. Gen. Psychiatry*, 48: 996– 1001.
- Benson MA, Newey SE, Martin-Rendon E, Hawkes R, and Blake DJ. (2001). Dysbindin,

- a novel coiled-coil containing protein that interacts with the dystrobrevins in muscle and brain. *J Biol Chem*, 276: 24232-24241.
- Benson MA, Sillitoe RV, Blake DJ. (2004). Schizophrenia genetics: dysbindin under the microscope. *Trends Neurosci.*, 27(9): 516-9.
- Bhardwaj SK, Baharnoori M, Sharif-Askari B, Kamath A, Williams S, and Srivastava LK. (2009). Behavioral characterization of dysbindin-1 deficient sandy mice. *Behav Brain Res.*, 197, 435-441.
- Bilder RM, Bogerts B, Ashtari M, Wu H, Alvir JM, Jody D, Reiter G, Bell L, Lieberman JA. (1995). Anterior hippocampal volume reductions predict frontal lobe dysfunction in first episode schizophrenia. *Schizophr Res.*, 17(1): 47-58
- Björkblom B, Ostman N, Hongisto V, Komarovski V, Filén JJ, Nyman TA, Kallunki T, Courtney MJ, Coffey ET. (2005). Constitutively active cytoplasmic c-Jun N-terminal kinase 1 is a dominant regulator of dendritic architecture: role of microtubule-associated protein 2 as an effector. *J Neurosci.*, 25(27): 6350-61.
- Boulland JL, Qureshi T, Seal RP, Rafiki A, Gundersen V, Bergersen LH, Fremeau RT Jr, Edwards RH, Storm-Mathisen J, Chaudhry FA. (2004). Expression of the vesicular glutamate transporters during development indicates the widespread corelease of multiple neurotransmitters. *J Comp Neurol.*, 480(3): 264-80.
- Burdick KE, Goldberg TE, Funke B, Bates JA, Lencz T, Kucherlapati R, and Malhotra AK. (2007). DTNBP1 genotype influences cognitive decline in schizophrenia. *Schizophr Res*, 89: 169-172.
- Burdick KE, Lencz T, Funke B, Finn CT, Szeszko PR, Kane JM, Kucherlapati R, and Malhotra AK. (2006). Genetic Variation in DTNBP1 Influences General Cognitive Ability. *Hum Mol Genet.*, 15(10): 1563-1568.

- Buzsaki G, Buhl DL, Harris KD, Csicsvari J, Czeh B, and Morozov A. (2003). Hippocampal network patterns of activity in the mouse. *Neuroscience*, 116: 201-211.
- Chao HT, Zoghbi HY, Rosenmund C. (2007). MeCP2 controls excitatory synaptic strength by regulating glutamatergic synapse number. *Neuron*, 56(1):58-65.
- Chen XW, Feng YQ, Hao CJ, Guo XL, He X, Zhou ZY, Guo N, Huang HP, Xiong W, Zheng H, Zuo PL, Zhang CX, Li W, and Zhou Z. (2008). DTNBP1, a schizophrenia susceptibility gene, affects kinetics of transmitter release. *J Cell Biol*, 181: 791-801.
- Chen M, Lucas KG, Akum BF, Balasingam G, Stawicki TM, Provost JM, Riefler GM, Jörnsten RJ, Firestein BL. (2005). A novel role for snapin in dendrite patterning: interaction with cypin. *Mol Biol Cell.*, 16(11): 5103-14.
- Coyle JT. (2006). Glutamate and schizophrenia: beyond the dopamine hypothesis. *Cell Mol Neurobiol.*, 26(4-6): 365-84.
- Cox MM, Tucker AM, Tang J, Talbot K, Richer DC, Yeh L, and Arnold SE. (2009). Neurobehavioral abnormalities in the dysbindin-1 mutant, sandy, on a C57BL/6J genetic background. *Genes Brain Behav*, 8: 390-397.
- Danbolt NC. (2001). Glutamate uptake. *Prog Neurobiol.*, 65(1): 1-105.
- d'Amato T, Rochet T, Dalery J, Laurent A, Chauchat JH, Terra JL, Marie-Cardine M. (1992). Relationship between symptoms rated with the Positive and Negative Syndrome Scale and brain measures in schizophrenia. *Psychiatry Res*, 44(1): 55-62.
- Donohoe G, Morris DW, Clarke S, McGhee KA, Schwaiger S, Nangle JM, Garavan H, Robertson IH, Gill M, and Corvin A. (2007). Variance in neurocognitive performance is associated with dysbindin-1 in schizophrenia: a preliminary study. *Neuropsychologia*, 45 : 454-458.
- Eastwood SL, Burnet PW, Harrison PJ. (1995). Altered synaptophysin expression as a

- marker of synaptic pathology in schizophrenia. *Neuroscience*, 66(2): 309-19.
- Eastwood SL, Harrison PJ. (2005). Decreased expression of vesicular glutamate transporter 1 and complexin II mRNAs in schizophrenia: further evidence for a synaptic pathology affecting glutamate neurons. *Schizophr Res.*, 73(2-3):159-72.
- Fannon D, Chitnis X, Doku V, Tennakoon L, O'Ceallaigh S, Soni W, Sumich A, Lowe J, Santamaria M, Sharma T. (2000). Features of structural brain abnormality detected in first-episode psychosis. *Am J Psychiatry*, 157(11): 1829-34.
- Fannon D, Tennakoon L, Sumich A, O'Ceallaigh S, Doku V, Chitnis X, Lowe J, Soni W, Sharma T. (2000). Third ventricle enlargement and developmental delay in first episode psychosis: preliminary findings. *Br J Psychiatry*, 177: 354-9.
- Feng YQ, Zhou ZY, He X, Wang H, Guo XL, Hao CJ, Guo Y, Zhen XC, and Li W. (2008). Dysbindin deficiency in sandy mice causes reduction of snapin and displays behaviors related to schizophrenia. *Schizophr Res*, 106: 218-228.
- Fonnum F. (1984). Glutamate: a neurotransmitter in mammalian brain. *J Neurochem*, 42: 1-11.
- Fremeau RT Jr, Kam K, Qureshi T, Johnson J, Copenhagen DR, Storm-Mathisen J, Chaudhry FA, Nicoll RA, Edwards RH. (2004). Vesicular glutamate transporters 1 and 2 target to functionally distinct synaptic release sites. *Science*, 304(5678):1815-9.
- Fremeau RT Jr, Troyer MD, Pahner I, Nygaard GO, Tran CH, Reimer RJ, *et al.* (2001). The expression of vesicular glutamate transporters defines two classes of excitatory synapse. *Neuron*, 31: 247-60.
- Fremeau RT Jr, Voglmaier S, Seal RP, Edwards RH. (2004). VGLUTs define subsets of excitatory neurons and suggest novel roles for glutamate. *Trends Neurosci.*, 27(2): 98-103.

- Garey LJ, Ong WY, Patel TS, Kanani M, Davis A, Mortimer AM, *et al.* (1998). Reduced dendritic spine density on cerebral cortical pyramidal neurons in schizophrenia. *J. Neurol., Neurosurg. Psychiatry*, 65: 446– 453.
- Gdalyahu A, Ghosh I, Levy T, Sapir T, Sapoznik S, Fishler Y, Azoulai D, Reiner O. (2004). DCX, a new mediator of the JNK pathway. *EMBO J.*, 23(4):823-32.
- Ghiani CA, Starcevic M, Rodriguez-Fernandez IA, Nazarian R, Cheli VT, Chan LN, Malvar JS, de Vellis J, Sabatti C, Dell'Angelica EC. (2010). The dysbindin-containing complex (BLOC-1) in brain: developmental regulation, interaction with SNARE proteins and role in neurite outgrowth. *Mol Psychiatry*, 115, 204-15.
- Gibb R, Kolb B. (1998). A method for vibratome sectioning of Golgi-Cox stained whole rat brain. *J Neurosci Methods*, 79(1): 1-4.
- Glantz LA, Lewis DA (2000). Decreased dendritic spine density on prefrontal cortical pyramidal neurons in schizophrenia. *Arch. Gen. Psychiatry*, 57: 65– 73.
- Goldman AL, Pezawas L, Mattay VS, Fischl B, Verchinski BA, Chen Q, Weinberger DR, Meyer-Lindenberg A. (2009). Widespread reductions of cortical thickness in schizophrenia and spectrum disorders and evidence of heritability. *Arch Gen Psychiatry*, 66(5): 467-77.
- Goutagny R, Jackson J, and Williams S. (2009). Self-generated theta oscillations in the hippocampus. *Nat Neurosci*, 12: 1491-1493.
- Grutzendler J, Kasthuri N, Gan WB. (2002). Long-term dendritic spine stability in the adult cortex. *Nature.*, 420(6917): 812-6.
- Harrison PJ. (1995). On the neuropathology of schizophrenia and its dementia: neurodevelopmental, neurodegenerative, or both? *Neurodegeneration*, 4(1): 1-12.
- Harrison PJ. (1996). Advances in post mortem molecular neurochemistry and

- neuropathology: examples from schizophrenia research. *Br Med Bull.*, 52(3): 527-38.
- Harrison PJ and Eastwood SL. (2003). Vesicular glutamate transporter (VGLUT1) gene expression provides further evidence for glutamatergic synaptic pathology in the hippocampus in schizophrenia [Abstract]. *Schizophr. Res.*, 60: 62-63.
- Hattori S, Murotani T, Matsuzaki S, Ishizuka T, Kumamoto N, Takeda M, Tohyama M, Yamatodani A, Kunugi H, and Hashimoto R. (2008). Behavioral abnormalities and dopamine reductions in *sd*y mutant mice with a deletion in *Dtnbp1*, a susceptibility gene for schizophrenia. *Biochem Biophys Res Commun*, 373: 298-302.
- Heckers S. (2001). Neuroimaging studies of the hippocampus in schizophrenia. *Hippocampus*, 11(5): 520-8.
- Heckers S, Rauch SL, Goff D, Savage CR, Schacter DL, Fischman AJ, Alpert NM. (1998). Impaired recruitment of the hippocampus during conscious recollection in schizophrenia. *Nat Neurosci.*, 1(4): 318-23.
- Holliday EG, Handoko HY, James MR, McGrath JJ, Nertney DA, Tirupati S, Thara R, Levinson DF, Hayward NK, Mowry BJ, Nyholt DR. (2006). Association study of the dystrobrevin-binding gene with schizophrenia in Australian and Indian samples. *Twin Res Hum Genet.*, 9(4): 531-9.
- Innocenti M, Gerboth S, Rottner K, Lai FP, Hertzog M, Stradal TE, Frittoli E, Didry D, Polo S, Disanza A, Benesch S, Di Fiore PP, Carlier MF, Scita G. (2005). *Abi1* regulates the activity of N-WASP and WAVE in distinct actin-based processes. *Nat Cell Biol*, 7(10): 969-76.
- Irwin SA, Galvez R, Greenough WT. (2000). Dendritic spine structural anomalies in fragile-X mental retardation syndrome. *Cereb Cortex*, 10(10): 1038-44.
- Ito H, Morishita R, Shinoda T, Iwamoto I, Sudo K, Okamoto K, Nagata K. (2010).

- Dysbindin-1, WAVE2 and Abi-1 form a complex that regulates dendritic spine formation. *Mol Psychiatry*, 15(10):976-86.
- Javitt DC.(2007). Glutamate and schizophrenia: phencyclidine, N-methyl-D-aspartate receptors, and dopamine-glutamate interactions. *Int Rev Neurobiol.*, 78: 69-108.
- Jentsch JD, Trantham-Davidson H, Jairl C, Tinsley M, Cannon TD, and Lavin A. (2009). Dysbindin modulates prefrontal cortical glutamatergic circuits and working memory function in mice. *Neuropsychopharmacology*, 34: 2601-2608.
- Joo EJ, Lee KY, Jeong SH, Ahn YM, Koo YJ, Kim YS. (2006). The dysbindin gene (DTNBP1) and schizophrenia: no support for an association in the Korean population. *Neurosci Lett.*, 407(2): 101-6
- Kahana MJ, Sekuler R, Caplan JB, Kirschen M, Madsen JR. (1999). Human theta oscillations exhibit task dependence during virtual maze navigation. *Nature*, 399(6738): 781-4.
- Kaibara T, Leung LS. (1993). Basal versus apical dendritic long-term potentiation of commissural afferents to hippocampal CA1: a current-source density study. *J Neurosci.*, 13(6): 2391-404
- Kalus P, Müller TJ, Zuschratter W, Senitz D. (2000). The dendritic architecture of prefrontal pyramidal neurons in schizophrenic patients. *Neuroreport.*, 11(16): 3621-5.
- Kawabe K, Miyamoto E.(2008). Effects of neonatal repeated MK-801 treatment on delayed nonmatching-to-position responses in rats. *Neuroreport.* 19(9): 969-73.
- Kelsoe JR Jr, Cadet JL, Pickar D, Weinberger DR. (1988). Quantitative neuroanatomy in schizophrenia. A controlled magnetic resonance imaging study. *Arch Gen Psychiatry*,45(6): 533-41
- Kendler KS. (2004). Schizophrenia genetics and dysbindin: a corner turned? *Am J*

- Psychiatry*, 161(9): 1533-6.
- Kirov G, Ivanov D, Williams NM, Preece A, Nikolov I, Milev R, Koleva S, Dimitrova A, Toncheva D, O'Donovan MC, Owen MJ. (2004). Strong evidence for association between the dystrobrevin binding protein 1 gene (DTNBP1) and schizophrenia in 488 parent offspring trios from Bulgaria. *Biol Psychiatry*, 55(10): 971-5.
- Kolluri N, Sun Z, Sampson AR, Lewis DA. (2005). Lamina-specific reductions in dendritic spine density in the prefrontal cortex of subjects with schizophrenia. *Am J Psychiatry*, 162(6):1200-2.
- Krystal JH, Karper LP, Seibyl JP, Freeman GK, Delaney R, Bremner JD, Heninger GR, Bowers MB Jr, Charney DS. (1994). Subanesthetic effects of the noncompetitive NMDA antagonist, ketamine, in humans. Psychotomimetic, perceptual, cognitive, and neuroendocrine responses. *Arch Gen Psychiatry*. 51(3): 199-214.
- Kuperberg GR, Broome MR, McGuire PK, David AS, Eddy M, Ozawa F, Goff D, West WC, Williams SC, van der Kouwe AJ, Salat DH, Dale AM, Fischl B. (2003). Regionally localized thinning of the cerebral cortex in schizophrenia. *Arch Gen Psychiatry*, 60(9): 878-88.
- Lieberman J, Chakos M, Wu H, Alvir J, Hoffman E, Robinson D, Bilder R. (2001). Longitudinal study of brain morphology in first episode schizophrenia. *Biol Psychiatry*, 49(6): 487-99.
- Leiderman E, Zylberman I, Zukin SR, Cooper TB, Javitt DC. (1996). Preliminary investigation of high-dose oral glycine on serum levels and negative symptoms in schizophrenia: an open-label trial. *Biol Psychiatry*, 39(3): 213-5.
- Li W, Zhang Q, Oiso N, Novak EK, Gautam R, O'Brien EP, Tinsley CL, Blake DJ, Spritz RA, Copeland NG, Jenkins NA, Amato D, Roe BA, Starcevic M,

- Dell'Angelica EC, Elliott RW, Mishra V, Kingsmore SF, Paylor RE, Swank RT. (2003). Hermansky-Pudlak syndrome type 7 (HPS7) results from mutant dysbindin, a member of the biogenesis of lysosome-related organelles complex 1 (BLOC-1). *Nat Genet*; 35: 84-89.
- Lui S, Deng W, Huang X, Jiang L, Ouyang L, Borgwardt SJ, Ma X, Li D, Zou L, Tang H, Chen H, Li T, McGuire P, Gong Q. (2009). Neuroanatomical differences between familial and sporadic schizophrenia and their parents: an optimized voxel-based morphometry study. *Psychiatry Res*, 171(2): 71-81.
- Manseau F, Danik M, Williams S. (2005). A functional glutamatergic neurone network in the medial septum and diagonal band area. *J Physiol.*, 566(Pt 3): 865-84.
- Masliah E, Terry RD, Alford M, DeTeresa R. (1990). Quantitative immunohistochemistry of synaptophysin in human neocortex: an alternative method to estimate density of presynaptic terminals in paraffin sections. *J Histochem Cytochem.*, 38(6): 837-44.
- McDonald C, Marshall N, Sham PC, Bullmore ET, Schulze K, Chapple B, Bramon E, Filbey F, Quraishi S, Walshe M, Murray RM. (2006). Regional brain morphometry in patients with schizophrenia or bipolar disorder and their unaffected relatives. *Am J Psychiatry*, 163(3): 478-87
- Meador-Woodruff JH, Healy DJ. (2000). Glutamate receptor expression in schizophrenic brain. *Brain Res Brain Res Rev.*, 31(2-3): 288-94
- Moriyama Y, Yamamoto A (2004). Glutamatergic chemical transmission: look! Here, there, and anywhere. *J Biochem.*, 135: 155-63.
- Morris D.W., McGhee K.A., Schwaiger S., Scully P., Quinn J., Meagher D., Waddington J.L., Gill M., and Corvin A.P. (2003). No evidence for association of the dysbindin

- gene [DTNBP1] with schizophrenia in an Irish population-based study. *Schizophr. Res.*, 60: 167-172.
- Murotani T, Ishizuka T, Hattori S, Hashimoto R, Matsuzaki S, Yamatodani A. (2007). High dopamine turnover in the brains of Sandy mice. *Neurosci Lett.*, 421(1): 47-51.
- Mutsuddi M, Morris DW, Waggoner SG, Daly MJ, Scolnick EM, Sklar P. (2006). Analysis of high-resolution HapMap of DTNBP1 (Dysbindin) suggests no consistency between reported common variant associations and schizophrenia. *Am J Hum Genet.*, 79(5): 903-9.
- Narayan VM, Narr KL, Kumari V, Woods RP, Thompson PM, Toga AW, Sharma T. (2007). Regional cortical thinning in subjects with violent antisocial personality disorder or schizophrenia. *Am J Psychiatry*, 164(9): 1418-27.
- Narr KL, Bilder RM, Toga AW, Woods RP, Rex DE, Szeszko PR, Robinson D, Sevy S, Gunduz-Bruce H, Wang YP, DeLuca H, Thompson PM. (2005). Mapping cortical thickness and gray matter concentration in first episode schizophrenia. *Cereb Cortex.*, 15(6): 708-19.
- Narr KL, Toga AW, Szeszko P, Thompson PM, Woods RP, Robinson D, Sevy S, Wang Y, Schrock K, Bilder RM. (2005). Cortical thinning in cingulate and occipital cortices in first episode schizophrenia. *Biol Psychiatry*, 58(1): 32-40.
- Navone F, Jahn R, Di Gioia G, Stukenbrok H, Greengard P, De Camilli P. (1986). Protein p38: an integral membrane protein specific for small vesicles of neurons and neuroendocrine cells. *J Cell Biol.*, 103(6 Pt 1): 2511-27.
- Nazarian R, Starcevic M, Spencer MJ, Dell'Angelica EC. (2006). Reinvestigation of the dysbindin subunit of BLOC-1 (biogenesis of lysosome-related organelles complex-1) as a dystrobrevin-binding protein. *Biochem J.*, 395(3): 587-98.

- Nelson MD, Saykin AJ, Flashman LA, Riordan HJ. (1998). Hippocampal volume reduction in schizophrenia as assessed by magnetic resonance imaging: a meta-analytic study. *Arch Gen Psychiatry*, 55(5): 433-40.
- Nesvåg R, Lawyer G, Varnäs K, Fjell AM, Walhovd KB, Frigessi A, Jönsson EG, Agartz I. (2008). Regional thinning of the cerebral cortex in schizophrenia: effects of diagnosis, age and antipsychotic medication. *Schizophr Res*, 98(1-3): 16-28.
- Numakawa T, Yagasaki Y, Ishimoto T, Okada T, Suzuki T, Iwata N, Ozaki N, Taguchi T, Tatsumi M, Kamijima K, Straub RE, Weinberger DR, Kunugi H, Hashimoto R. (2004). Evidence of novel neuronal functions of dysbindin, a susceptibility gene for schizophrenia. *Hum. Mol. Genet.*, 13: 2699-2708.
- Owen MJ, Williams NM, O'Donovan MC. (2004). Dysbindin-1 and schizophrenia: from genetics to neuropathology. *J Clin Invest.*, 113(9): 1255-7.
- Pak CW, Flynn KC, Bamberg JR. (2008). Actin-binding proteins take the reins in growth cones. *Nat Rev Neurosci.*, 9(2): 136-47.
- Park M, Salgado JM, Ostroff L, Helton TD, Robinson CG, Harris KM, Ehlers MD. (2006). Plasticity-induced growth of dendritic spines by exocytic trafficking from recycling endosomes. *Neuron*, 52(5): 817-30.
- Peters K, Wiltshire S, Henders AK, Dragović M, Badcock JC, Chandler D, Howell S, Ellis C, Bouwer S, Montgomery GW, Palmer LJ, Kalaydjieva L, Jablensky A (2008). Comprehensive analysis of tagging sequence variants in DTNBP1 shows no association with schizophrenia or with its composite neurocognitive endophenotypes. *Am J Med Genet B Neuropsychiatr Genet.*, 147B(7): 1159-66.
- Pennington K, Dicker P, Hudson L, Cotter DR (2008) Evidence for reduced neuronal somal size within the insular cortex in schizophrenia, but not in affective disorders.

- Schizophr Res.*, 106: 164-171.
- Pierri JN, Volk CL, Auh S, Sampson A, Lewis DA. (2001). Decreased somal size of deep layer 3 pyramidal neurons in the prefrontal cortex of subjects with schizophrenia. *Arch. Gen. Psychiatry*, 58: 466–473.
- Prescott CA and Gottesman II. (1993). Genetically mediated vulnerability to schizophrenia, *Psychiatr. Clin. North Am.*, 16: 245-267.
- Proepper C, Johannsen S, Liebau S, Dahl J, Vaida B, Bockmann J, Kreutz MR, Gundelfinger ED, Boeckers TM. (2007). Abelson interacting protein 1 (Abi-1) is essential for dendrite morphogenesis and synapse formation. *EMBO J*, 26(5):1397-409.
- Schultz CC, Koch K, Wagner G, Roebel M, Nenadic I, Schachtzabel C, Reichenbach JR, Sauer H, Schlösser RG. (2010). Complex pattern of cortical thinning in schizophrenia: results from an automated surface based analysis of cortical thickness. *Psychiatry Res.*, 182(2): 134-40.
- Schwab SG, Knapp M, Mondabon S, Hallmayer J, Borrmann-Hassenbach M, Albus M, Lerer B, Rietschel M, Trixler M, Maier W, Wildenauer DB. (2003). Support for association of schizophrenia with genetic variation in the 6p22.3 gene, dysbindin, in sib-pair families with linkage and in an additional sample of triad families. *Am J Hum Genet.*, 72(1): 185-90.
- Seal RP, Edwards RH. (2006). The diverse roles of vesicular glutamate transporter 3. *Handb Exp Pharmacol.*, 137-50.
- Sekino Y, Kojima N, Shirao T. (2007). Role of actin cytoskeleton in dendritic spine morphogenesis. *Neurochem Int.*, 51(2-4): 92-104.

- Selemon LD, Mrzljak J, Kleinman JE, Herman MM, Goldman-Rakic PS. (2003). Regional specificity in the neuropathologic substrates of schizophrenia: a morphometric analysis of Broca's area 44 and area 9. *Arch Gen Psychiatry*, 60(1): 69-77.
- Selemon LD, Rajkowska G, Goldman-Rakic PS. (1995). Abnormally high neuronal density in the schizophrenic cortex. A morphometric analysis of prefrontal area 9 and occipital area 17. *Arch Gen Psychiatry*, 805-18; discussion 819-20.
- Shenton ME, Dickey CC, Frumin M, McCarley RW. (2001). A review of MRI findings in schizophrenia. *Schizophr Res.*, 49(1-2): 1-52.
- Silverman JM, Smith CJ, Guo SL, Mohs RC, Siever LJ, Davis KL. (1998). Lateral ventricular enlargement in schizophrenic probands and their siblings with schizophrenia-related disorders. *Biol Psychiatry*, 43(2): 97-106.
- Soderling SH, Guire ES, Kaech S, White J, Zhang F, Schutz K, Langeberg LK, Banker G, Raber J, Scott JD. (2007). A WAVE-1 and WRP signaling complex regulates spine density, synaptic plasticity, and memory. *J Neurosci.*, 27(2): 355-65.
- Stark AK, Uylings HB, Sanz-Arigita E, Pakkenberg B. (2004). Glial cell loss in the anterior cingulate cortex, a subregion of the prefrontal cortex, in subjects with schizophrenia. *Am J Psychiatry*, 161(5): 882-8.
- Südhof TC, Lottspeich F, Greengard P, Mehl E, Jahn R. (1987). "The cDNA and derived amino acid sequences for rat and human synaptophysin". *Nucleic Acids Res.*, **15** (22): 9607.
- Sumich A, Chitnis XA, Fannon DG, O'Ceallaigh S, Doku VC, Falrowicz A, Marshall N, Matthew VM, Potter M, Sharma T. (2002). Temporal lobe abnormalities in first episode psychosis. *Am J Psychiatry*, 159(7): 1232-5.

Swank R.T., Sweet H.O., Davisson M.T., Reddington M., and Novak E.K. (1991).

Sandy: a new mouse model for platelet storage pool deficiency, *Genet. Res.*, 58: 51-62.

Sweet RA, Henteleff RA, Zhang W, Sampson AR, Lewis DA. (2009). Reduced dendritic spine density in auditory cortex of subjects with schizophrenia.

Neuropsychopharmacology, 34(2):374-89.

Sweet RA, Pierri JN, Auh S, Sampson AR, Lewis DA. (2003). Reduced pyramidal cell somal volume in auditory association cortex of subjects with schizophrenia.

Neuropsychopharmacology. 28(3):599-609.

Takamori S, Rhee JS, Rosenmund C, Jahn R. (2000). Identification of a vesicular glutamate transporter that defines a glutamatergic phenotype in neurons. *Nature*, 407: 189–94.

Takao K, Toyama K, Nakanishi K, Hattori S, Takamura H, Takeda M, Miyakawa T, and Hashimoto R. (2008). Impaired long-term memory retention and working memory in *sd*y mutant mice with a deletion in *Dtnbp1*, a susceptibility gene for schizophrenia.

Mol Brain, 1(1): 11.

Talbot K, Cho DS, Ong WY, Benson MA, Han LY, Kazi HA, Kamins J, Hahn CG, Blake DJ, and Arnold SE. (2006). Dysbindin-1 is a synaptic and microtubular protein that binds brain snapin. *Hum Mol Genet*, 15: 3041-3054.

Talbot K, Eidem WL, Tinsley CL, Benson MA, Thompson EW, Smith RJ, Hahn CG, Siegel SJ, Trojanowski JQ, Gur RE, Blake DJ, and Arnold SE. (2004). Dysbindin-1 is reduced in intrinsic, glutamatergic terminals of the hippocampal formation in schizophrenia, *J. Clin. Invest*; 113: 1353-1363.

Talbot K, Ong WY, Blake DJ *et al.* (2009). Dysbindin-1 and its protein family. In: Javitt

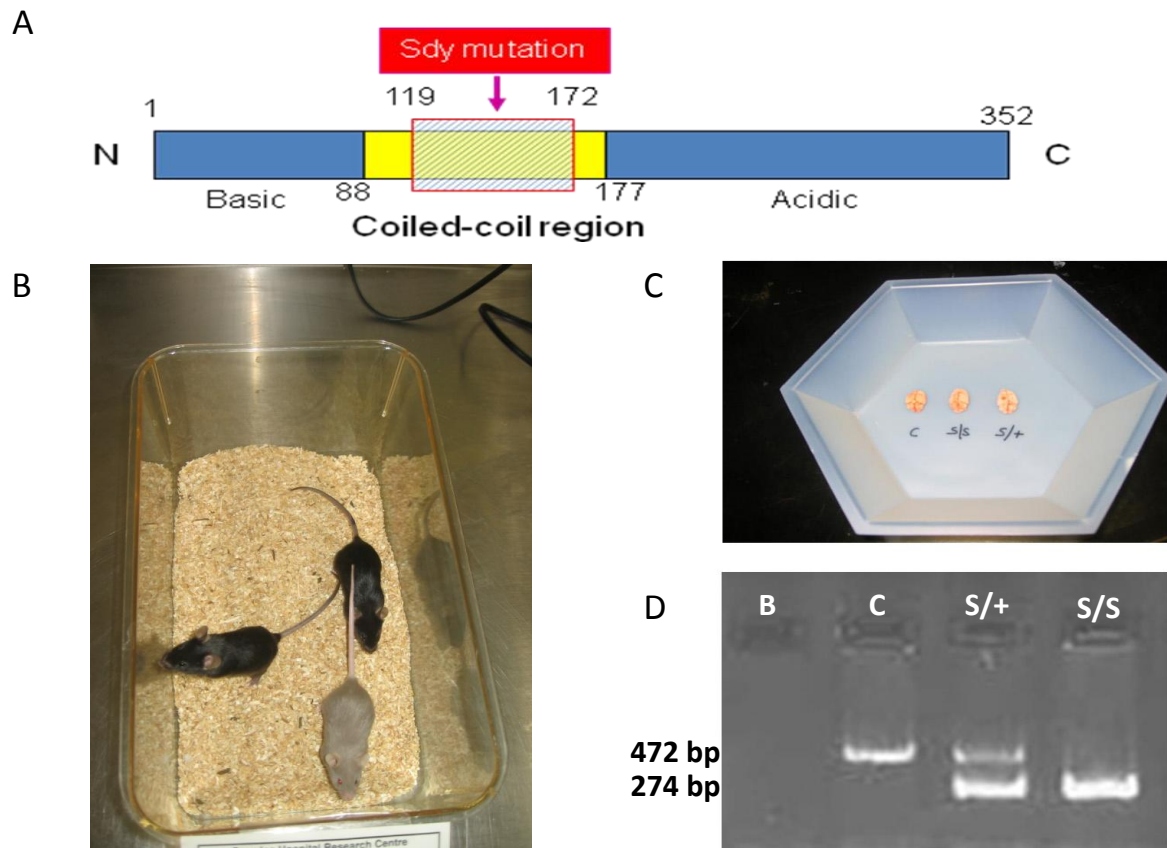
- DC, Kantrowitz J (eds). *Handbook of Neurochemistry and Molecular Neurobiology*, 3rd, 27, 107- 241, New York: Springer Science.
- Tang TT, Yang F, Chen BS, Lu Y, Ji Y, Roche KW, and Lu B. (2009). Dysbindin regulates hippocampal LTP by controlling NMDA receptor surface expression. *Proc Natl Acad Sci U S A*, 106: 21395-21400.
- Tang J.X., Zhou J., Fan J.B., Li X.W., Shi Y.Y., Gu N.F., Feng G.Y., Xing Y.L., Shi J.G., and He L. (2003). Family-based association study of DTNBP1 in 6p22.3 and schizophrenia. *Mol Psychiatry*, 8 : 717-718.
- Tochigi M, Zhang X, Ohashi J, Hibino H, Otowa T, Rogers M, Kato T, Okazaki Y, Kato N, Tokunaga K, Sasaki T. (2006). Association study of the dysbindin (DTNBP1) gene in schizophrenia from the Japanese population. *Neurosci Res.*, 56(2): 154-8.
- Trachtenberg JT, Chen BE, Knott GW, Feng G, Sanes JR, Welker E, Svoboda K. (2002). Long-term in vivo imaging of experience-dependent synaptic plasticity in adult cortex. *Nature*, 420(6917): 788-94.
- Tsuang MT, Stone WS, Faraone SV. (2001). Genes, environment and schizophrenia. *Br J Psychiatry Suppl.*, 40: s18-24.
- Rajkowska G, Selemon LD, Goldman-Rakic PS. (1998). Neuronal and glial somal size in the prefrontal cortex. *Arch. Gen. Psychiatry*, 55: 215–224.
- Rosoklija G, Toomayan G, Ellis SP, Keilp J, Mann JJ, Latov N, Hays AP, Dwork AJ. (2000). Structural abnormalities of subicular dendrites in subjects with schizophrenia and mood disorders: preliminary findings. *Arch Gen Psychiatry*, 57(4): 349-56.
- Saha S, Chant D, Welham J, McGrath J (2005) A systematic review of the prevalence of schizophrenia. *PLoS Med* 2: e141.
- Sullivan PF, Kendler KS, Neale MC. (2003). Schizophrenia as a complex trait: evidence

- from a meta- analysis of twin studies. *Arch Gen Psychiatry*. 60(12): 1187-92.
- Straub RE, Jiang Y, MacLean CJ, Ma Y, Webb BT, Myakishev MV, Harris-Kerr C, Wormley B, Sadek H, Kadambi B, Cesare AJ, Gibberman A, Wang X, O'Neill FA, Walsh D, Kendler KS.(2002). Genetic variation in the 6p22.3 gene DTNBP1, the human ortholog of the mouse dysbindin gene, is associated with schizophrenia. *Am J Hum Genet.*, 71(2): 337-48.
- Straub RE, MacLean CJ, O'Neill FA, Burke J, Murphy B, Duke F, Shinkwin R, Webb BT, Zhang J, Walsh D, *et al.* (1995). A potential vulnerability locus for schizophrenia on chromosome 6p24-22: evidence for genetic heterogeneity. *Nat Genet.*, 11(3): 287-93.
- Van Den Bogaert A, Schumacher J, Schulze TG, Otte AC, Ohlraun S, Kovalenko S, Becker T, Freudenberg J, Jönsson EG, Mattila-Evenden M, Sedvall GC, Czerski P.M, Kapelski P, Hauser J, Maier W, Rietschel M, Propping P, Nöthen MM, Cichon S (2003). The DTNBP1 (dysbindin) gene contributes to schizophrenia, depending on family history of the disease. *Am J Hum Genet.*, 73(6): 1438-43.
- van den Oord EJ, Sullivan PF, Jiang Y, Walsh D, O'Neill FA, Kendler KS, Riley BP. Identification of a high-risk haplotype for the dystrobrevin binding protein 1 (DTNBP1) gene in the Irish study of high-density schizophrenia families. (2003). *Mol Psychiatry.*, 8(5): 499-510.
- van der Staay FJ, Arndt SS, Nordquist RE (2009) Evaluation of animal models of neurobehavioral disorders. *Behav Brain Funct.*, 5: 11.
- Velakoulis D, Pantelis C, McGorry PD, Dudgeon P, Brewer W, Cook M, Desmond P, Bridle N, Tierney P, Murrie V, Singh B, Copolov D. (1999). Hippocampal volume in first-episode psychoses and chronic schizophrenia: a high-resolution magnetic

- resonance imaging study. *Arch Gen Psychiatry*. 56(2): 133-41.
- Venkatasubramanian G, Jayakumar PN, Gangadhar BN, Keshavan MS. (2008). Automated MRI parcellation study of regional volume and thickness of prefrontal cortex (PFC) in antipsychotic-naïve schizophrenia. *Acta Psychiatr Scand.*, 117(6): 420-31.
- Wallén-Mackenzie A, Wootz H, Englund H. (2010). Genetic inactivation of the vesicular glutamate transporter 2 (VGLUT2) in the mouse: what have we learnt about functional glutamatergic neurotransmission? *Ups J Med Sci.*, 115(1): 11-20.
- Weickert CS, Straub RE, McClintock BW, Matsumoto M, Hashimoto R, Hyde TM, Herman MM, Weinberger DR, and Kleinman JE. (2004). Human dysbindin (DTNBP1) gene expression in normal brain and in schizophrenic prefrontal cortex and midbrain. *Arch Gen Psychiatry*, 61, 544-555.
- Weinberger DR. (1995). From neuropathology to neurodevelopment. *Lancet*, 346: 552-557.
- Weinberger DR. (1996). On the plausibility of "the neurodevelopmental hypothesis" of schizophrenia. *Neuropsychopharmacology.*, 14(3 Suppl): 1S-11S.
- Whitworth AB, Kemmler G, Honeder M, Kremser C, Felber S, Hausmann A, Walch T, Wanko C, Weiss EM, Stuppaeck CH, Fleischhacker WW. (2005). Longitudinal volumetric MRI study in first- and multiple-episode male schizophrenia patients. *Psychiatry Res.*, 30; 140(3): 225-37.
- Williams NM, O'Donovan MC, Owen MJ. (2005). Is the dysbindin gene (DTNBP1) a Susceptibility gene for schizophrenia? *Schizophr Bull.*, 31(4): 800-5.
- Yurgelun-Todd DA, Coyle JT, Gruber SA, Renshaw PF, Silveri MM, Amico E, Cohen B, Goff DC. (2005). Functional magnetic resonance imaging studies of schizophrenic

patients during word production: effects of D-cycloserine. *Psychiatry Res.*,138(1): 23-31.

Yu-Yen Ip E., Giza CC, Griesbach GS, Hovda DA. (2002). Effects of enriched environment and fluid percussion injury on dendritic arborization within the cerebral cortex of the developing rat. *Journal of Neurotrauma*, 19(5): 573-585

Figure 1. Dysbindin-1 gene mutation and sandy mice.

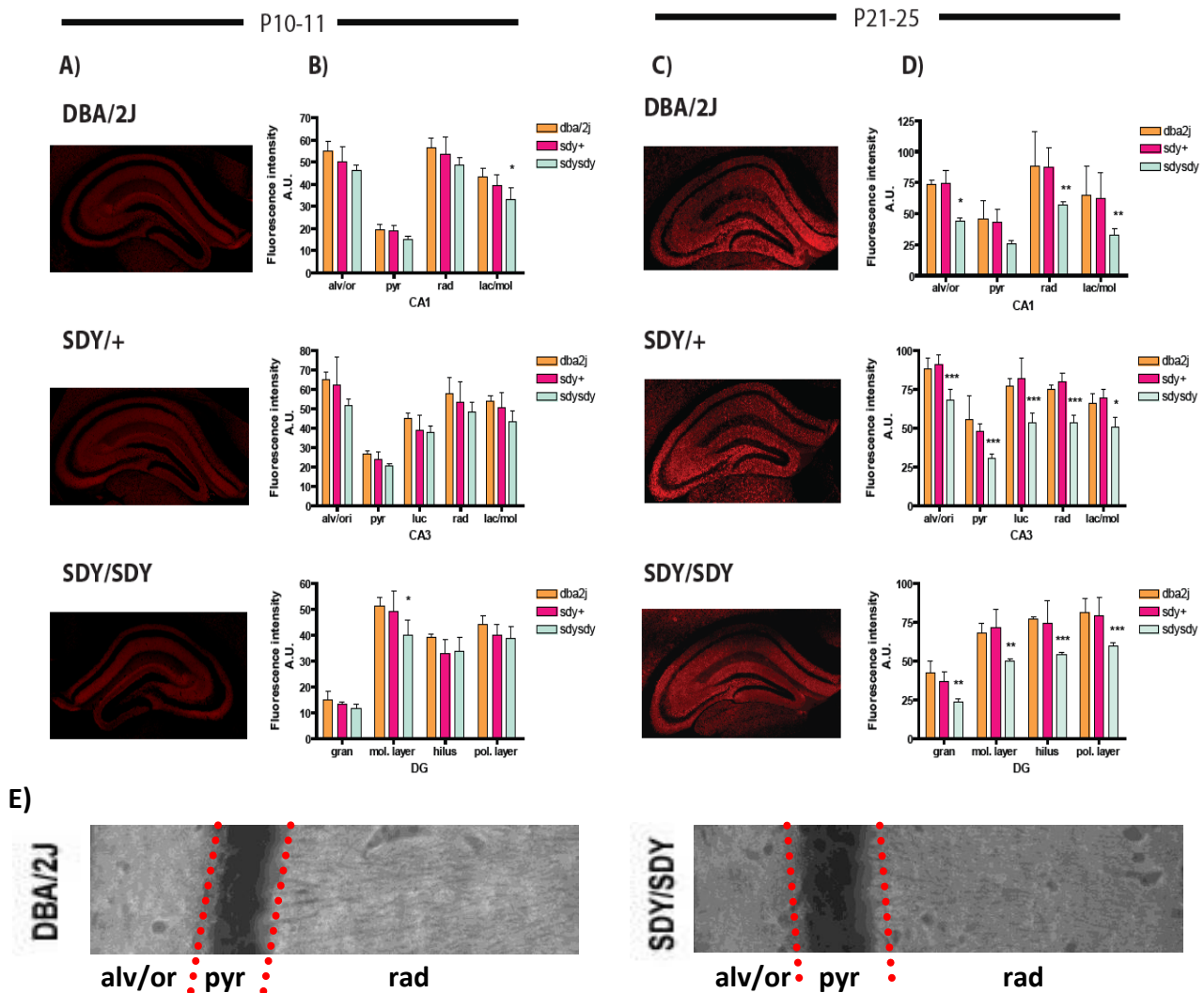
A. Structure of mouse dysbindin-1 gene and sdy mutation.

B. Picture of an adult sdy/sdy homozygous (grey, foreground), a sdy/+ heterozygous (black, in the left) and a wild-type control (black, in the back). The size and body weights are comparable to controls. Sandy mice show apparently normal cage behavior, that is, movement within the cage, feeding and drinking pattern, and interactions with control mice.

C. Fresh frozen brains of a wild-type control (C), sdy/sdy (s/s) and sdy/+ (s/+). The surface morphology of brains of sandy mutants looks apparently normal and comparable to controls in terms of gross appearance and weight. Left: control brain (0.3955 g), middle, sdy/sdy (0.412 g), right, sdy/+ (0.4122 g).

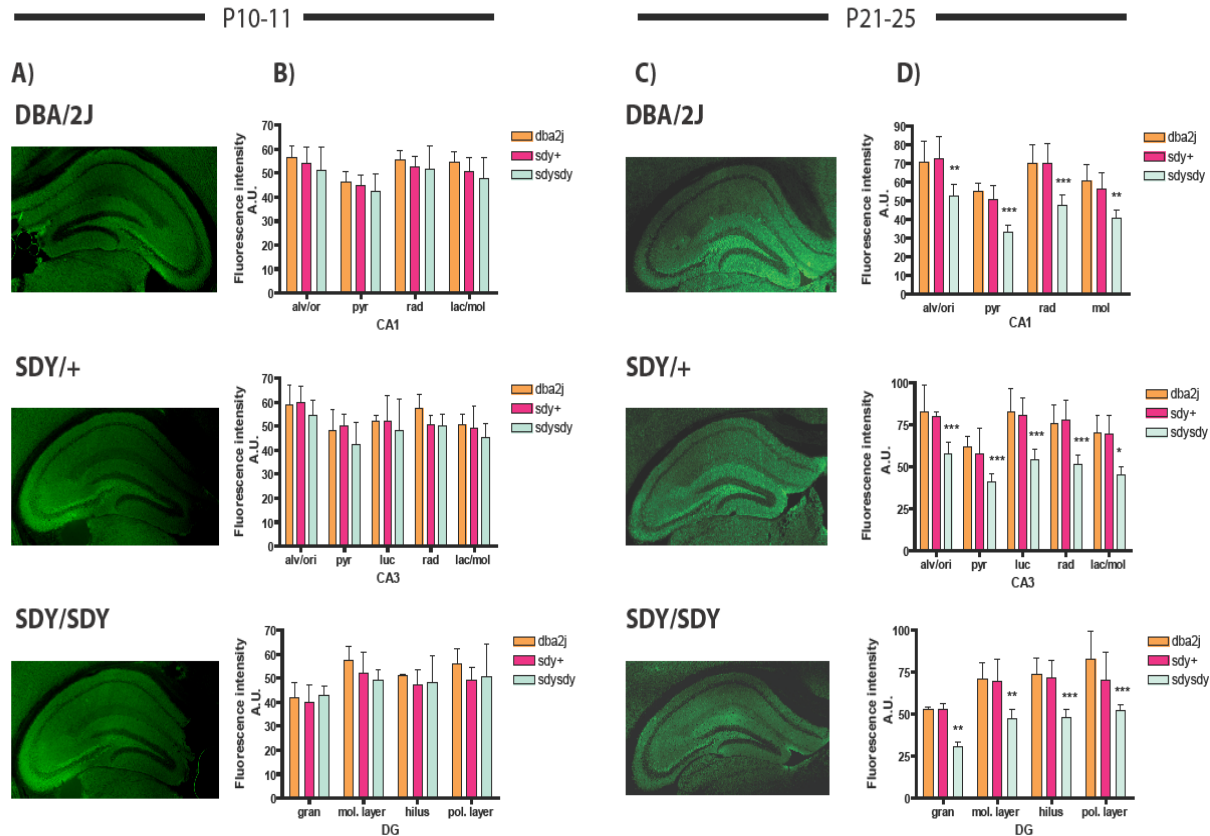
D. The mice will be genotyped using a PCR procedure designed to yield PCR products across the segment of *Dtnbp1* deleted in sdy mice as originally reported by Li *et al.* (2003). A 472 base pair PCR product is yielded from the wild-type gene and a 274 base pair PCR product is yielded from the sdy gene. The 472 base pair product is detected in wild-type and sdy/+ mice whereas the 274 base pair product is selectively detected in sdy/+ and sdy/sdy mice. Picture of PCR product on 2% agarose gel for negative control (B), control (C), heterozygous sdy/+ (s/+) and homozygous sdy/sdy (s/s).

Figure 2. Immunohistochemistry of vGLUT1 in the hippocampal subregions of control DBA/2J, *sdyl/+* and *sdyl/sdy* mice



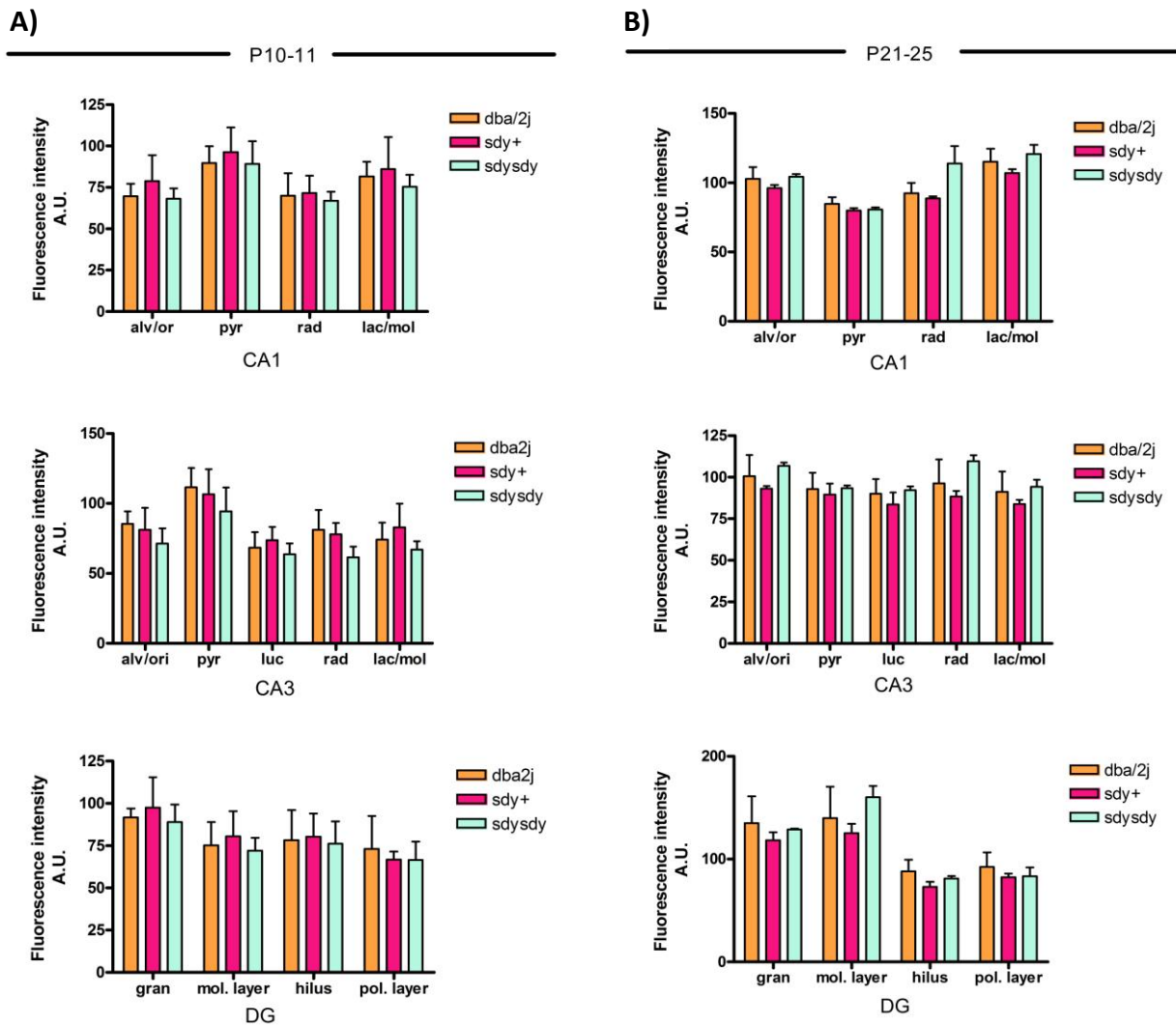
A) Representative images of hippocampal sections used, from the P10-11 DBA/2J (top), the heterozygous (middle) and the homozygous (bottom) mice group. B) Quantitative analysis of the fluorescent intensity over representative area in the different layers of the hippocampus. A significant decrease was observed in the mol. layer in *sdyl/sdy* (*: $p < 0.05$) (DBA/2J, *sdyl/+* and *sdyl/sdy* $n = 3$, five sections were analyzed per animals and averaged). C) Representative images of hippocampal sections used, from the P21-25 DBA/2J (top), the heterozygous (middle) and the homozygous (bottom) mice group. D) Quantitative analysis of the fluorescent intensity over representative area in the different layers of the hippocampus. A significant decrease was observed in *sdyl/sdy* across all subregions of the CA1, CA3 and DG (*: $p < 0.05$; **: $p < 0.01$; ***: $p < 0.001$) and CA3 ($p = 0.0283$) (DBA/2J, *sdyl/+* and *sdyl/sdy* $n = 5$, five sections were analyzed per animals and averaged). E) Representative fluorescence micrographs of CA1 subregional immunohistochemical against vGLUT1 at PD21-25 from DBA/2J and *sdyl/sdy* (40x magnitude).

Figure 4. Immunohistochemistry of synaptophysin in the hippocampal subregions of control DBA/2J, *sdyl/+* and *sdyl/sdy* mice



A) Representative images of hippocampal sections used, from the P10-11 DBA/2J (top), the heterozygous (middle) and the homozygous (bottom) mice group. B) Quantitative analysis of the fluorescent intensity over representative area in the different layers of the hippocampus. No significant decrease was observed across all subregions of hippocampus (DBA/2J, *sdyl/+* and *sdyl/sdy* $n = 3$, five sections were analyzed per animals and averaged). C) Representative images of hippocampal sections used, from the P21-25 DBA/2J (top), the heterozygous (middle) and the homozygous (bottom) mice group. D) Quantitative analysis of the fluorescent intensity over representative area in the different layers of the hippocampus. A significant decrease was observed in *sdyl/sdy* across all subregions of the CA1, CA3 and DG (*: $p < 0.05$; **: $p < 0.01$; ***: $p < 0.001$) and CA3 ($p = 0.0283$) (DBA/2J, *sdyl/+* and *sdyl/sdy* $n = 5$, five sections were analyzed per animals and averaged)

Figure 6. Immunohistochemistry of vGAT in the hippocampal subregions of control DBA/2J, *sdyl*+ and *sdyl*/*sdyl* mice

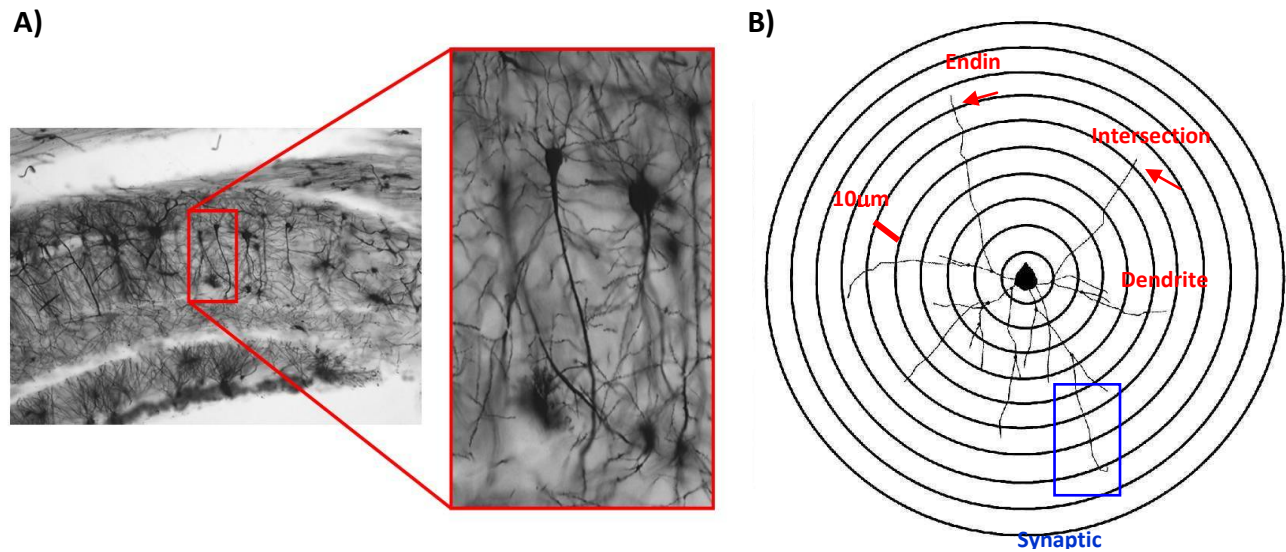


A) Quantitative analysis of the fluorescent intensity over representative area in the different layers of the hippocampus. No significant decrease was observed across all subregions of hippocampus (DBA/2J, *sdyl*+ and *sdyl*/*sdyl* $n=3$, five sections were analyzed per animals and averaged). B) Quantitative analysis of the fluorescent intensity over representative area in the different layers of the hippocampus. No significant decrease was observed across all subregions of the CA1, CA3 and DG (DBA/2J, *sdyl*+ and *sdyl*/*sdyl* $n=5$, five sections were analyzed per animals and averaged).

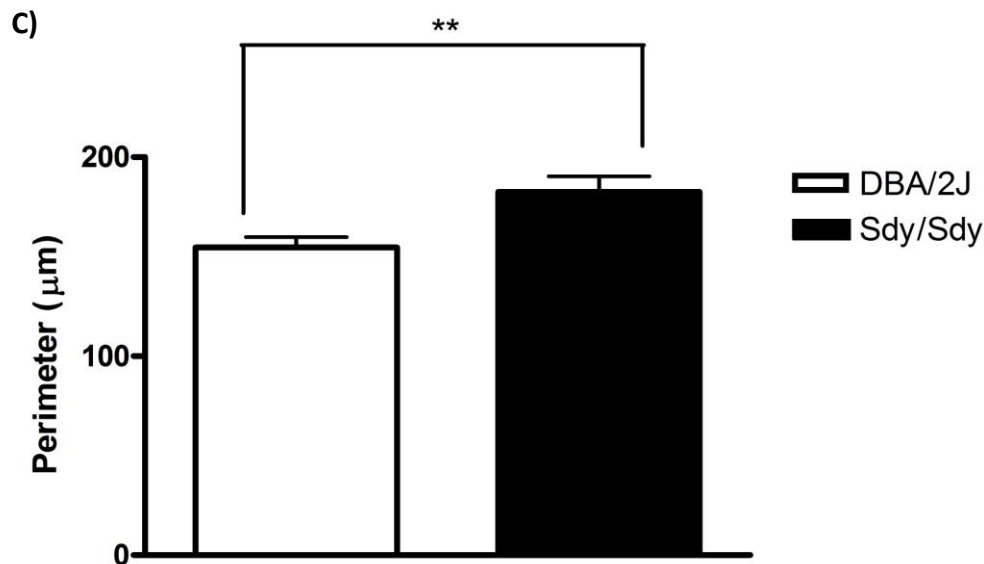
Table 1. Summary of immunohistochemistry findings

Fluorescent markers	Post-natal day 10-11	Post-natal day 21-25
vGLUT 1 (vesicular)	↓ in molecular layer of dentate gyrus of s/s	↓ all subregions of hippocampus of s/s
vGLUT 2 (vesicular)	↓ all subregions of hippocampus of s/s	No difference
vGAT (vesicular)	No difference	No difference
Synaptophysin (vesicular)	No difference	↓ all subregions of hippocampus of s/s
Syntaxin-1A (pre-synaptic membrane)	No difference	No difference

Summary of quantitative analysis of the vGLUT1/2, vGAT, synaptophysin and syntaxin 1-A fluorescent intensity over representative area in the different layers of the hippocampus as presented in figure 2-6.

Figure 7. Modified Golgi-Cox staining of CA1 pyramidal neurons.

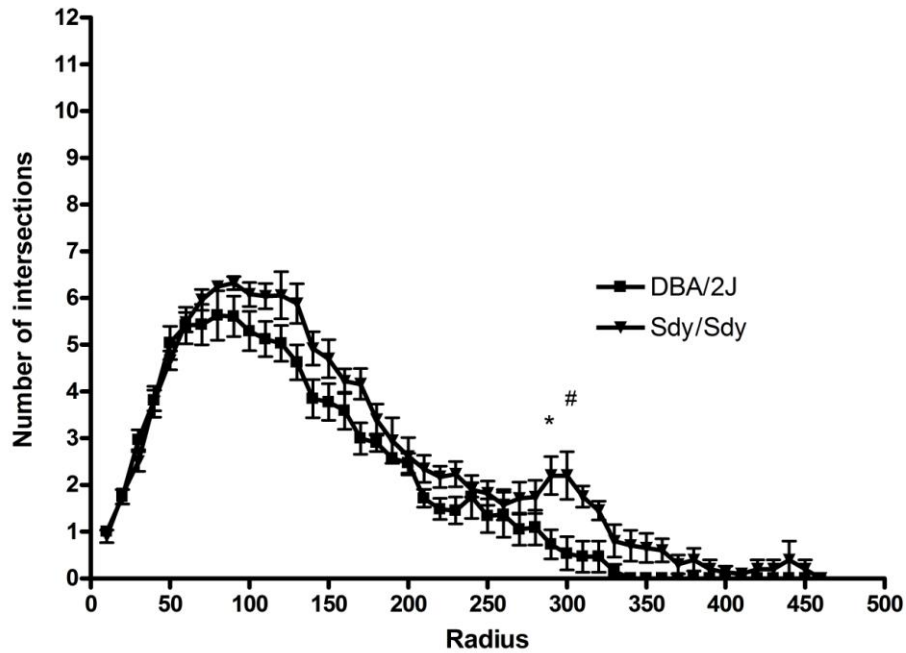
(Modified from, Emily Yu Yen, *J Neurotrauma*; May 2002)



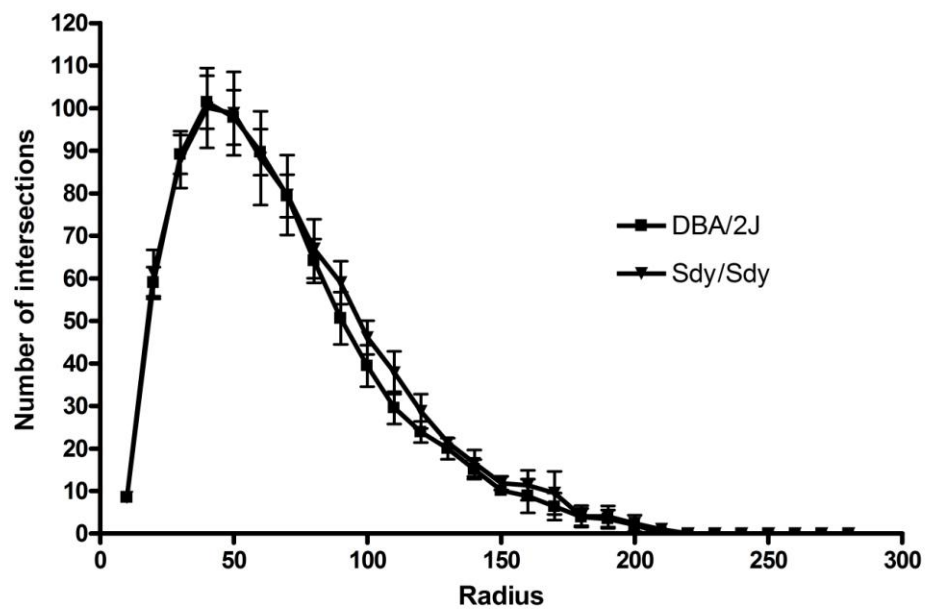
A) Representative photomicrographs of Golgi-Cox impregnated CA1 pyramidal neurons at PD60. B) The number of dendritic branching was assessed by Sholl analysis by counting the number of intersections on an overlay of concentric rings (10 μm interval between rings) surrounding the neuronal soma. The total length of dendrites across all concentric rings was also calculated by Sholl analysis using NeuroLucida system. For spine density measurements, one terminal dendrite from the third order tip (minimum length 20 μm) of each selected neuron was used to count spines at a magnification of 100X. The results are expressed as number of spines/10 μm . C) Soma size analysis. Significant increase in cell diameter was observed in sdy/sdy as compared to W/T. (**: $p < 0.01$)

Figure 8. Apical and basilar dendritic arborization of CA1 neurons

A)



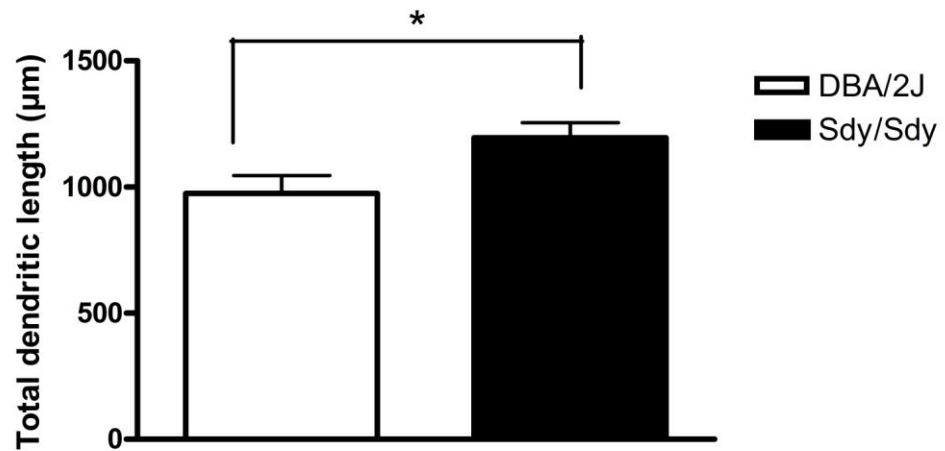
B)



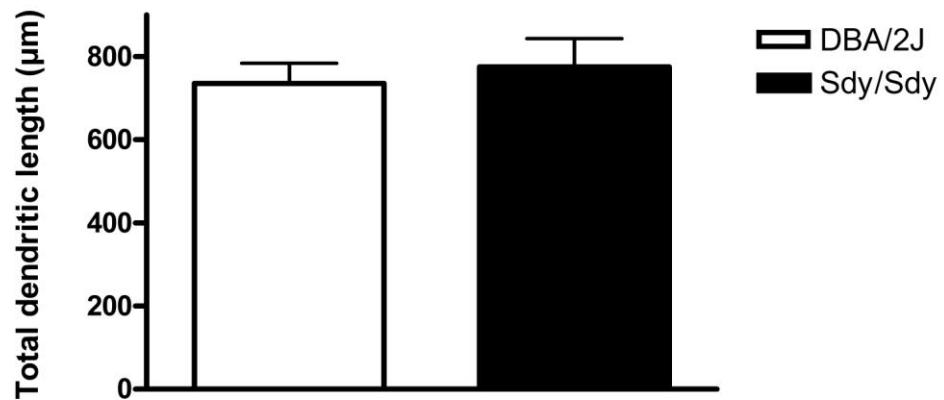
A) Apical dendrites arborization. B) Basilar dendritic arborization. Number of dendritic intersections per each shell radius (10µm). ANOVA revealed significant main effect of genotype. (*: $p < 0.05$; #: $p < 0.01$) in distal apical dendritic tree.

Figure 9. Apical and basilar total dendritic length of CA1 neurons

A)



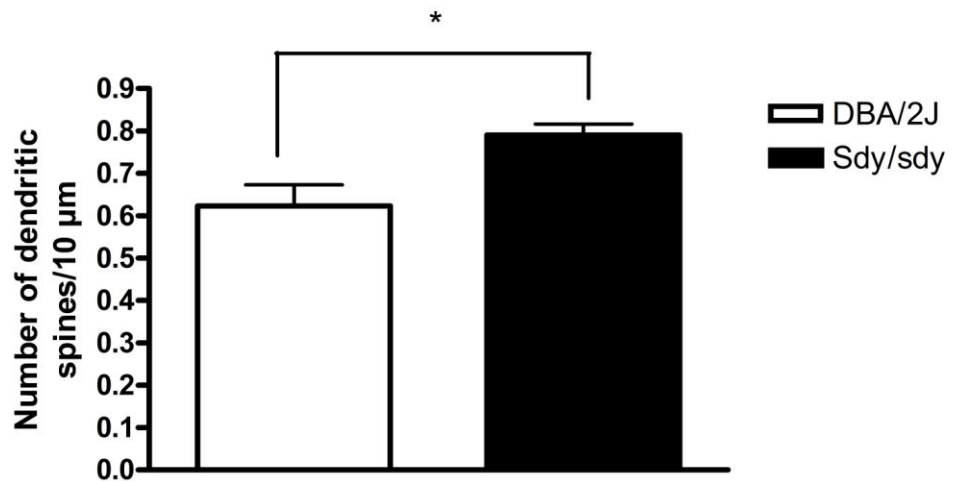
B)



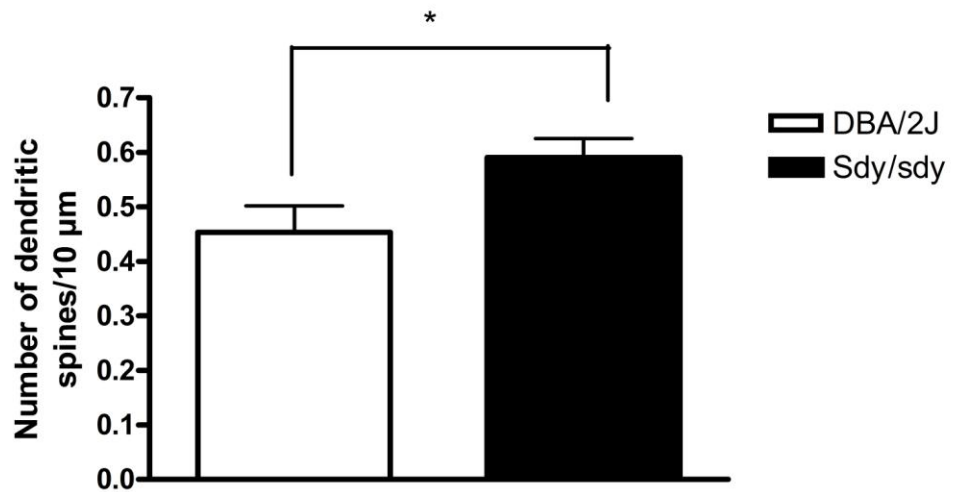
A. Apical dendrite. B. Basilar dendrite. Significant increase was observed in apical dendrites of *sdj/+* as compared to DBA/2J (*: $p < 0.05$).

Figure 10. Apical and basilar total spine density of CA1 neurons.

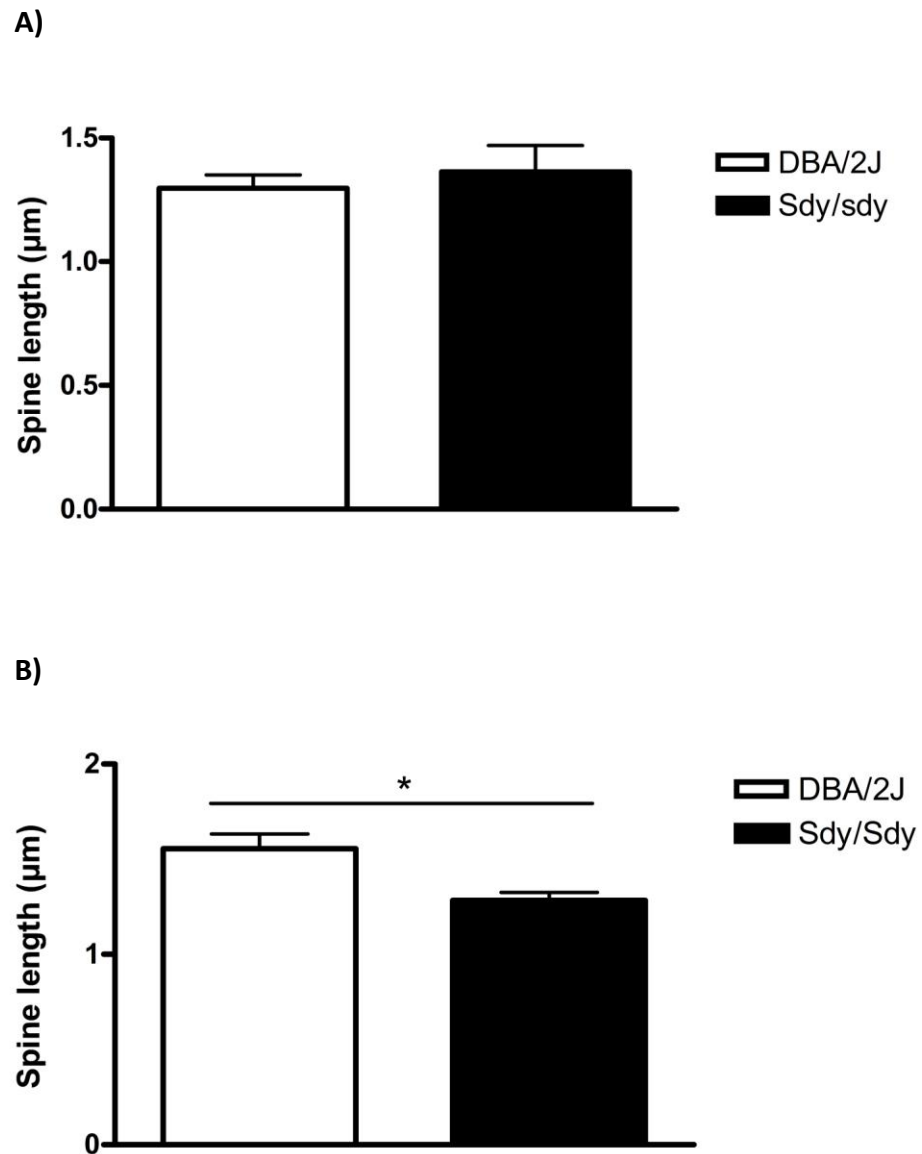
A)



B)



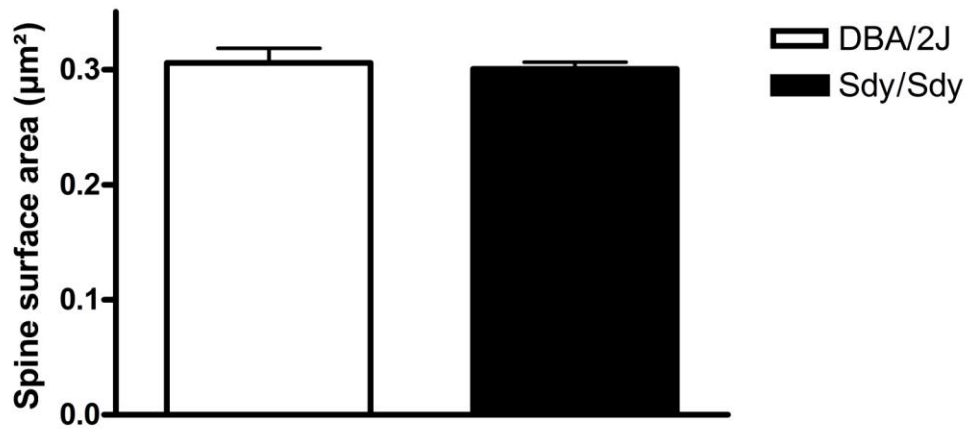
A. Apical dendrite. B. Basilar dendrite. Significant increase was observed in basilar dendrites in *sdj/+* as compared to DBA/2J. (*: $p < 0.05$).

Figure 11. Apical and basilar total spine length of CA1 neurons.

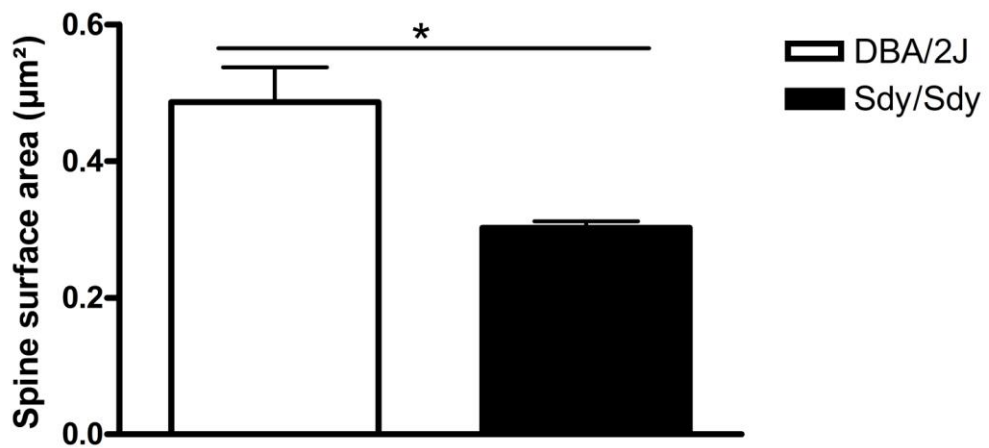
A. Apical dendrite. B. Basilar dendrite. Significant decrease was observed in spine length of basilar dendrites in sdy/sdy as compared to DBA/2J (*: $p < 0.05$).

Figure 12. Apical and basilar total spine surface of CA1 neurons.

A)



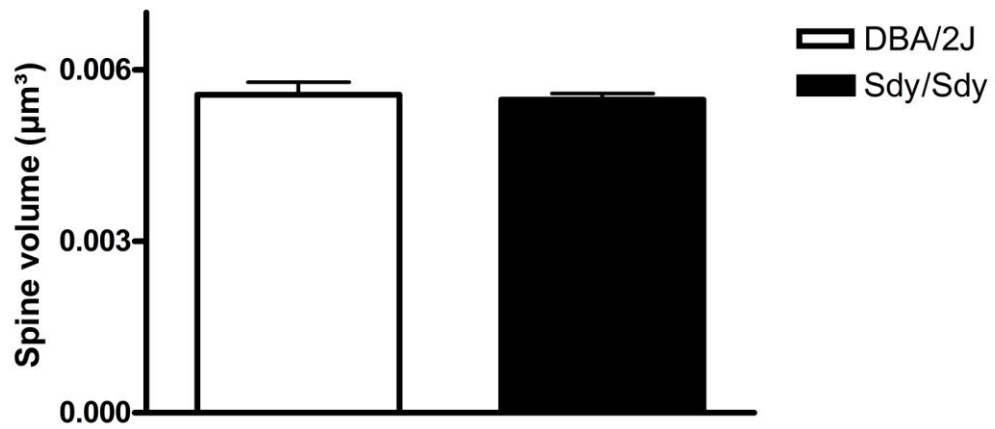
B)



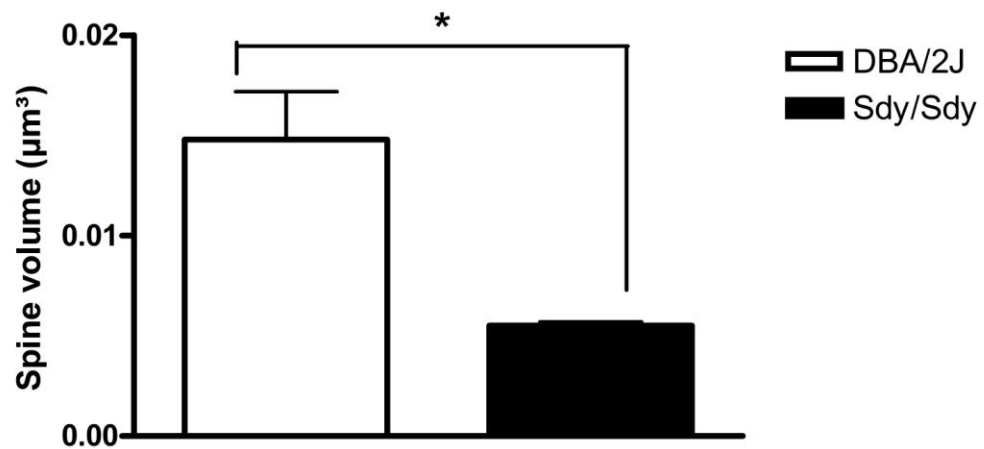
A. Apical dendrite. B. Basilar dendrite. Significant decrease was observed in basilar dendrites of sdy/sdy as compared to DBA/2J (*: $p < 0.05$).

Figure 13. Apical and basilar total spine volume of CA1 neurons.

A)



B)



A. Apical dendrite. B. Basilar dendrite. Significant decrease was observed in basilar dendrites of sdy/sdy as compared to DBA/2J (*: $p < 0.05$).

Table 2. Summary of morphological findings

	Apical	Basilar
Soma size	 in s/+ and s/s as compared to DBA/2J	
Dendritic arborization	 in s/+	
Spine density		 in s/+
Spine length		 in s/s
Spine surface		 in s/s
Spine volume		 in s/s

Summary of analysis of CA1 neuronal morphological changes in soma size, apical and basilar dendritic arborization, spine density and spine structure (length, surface and volume) as presented in figure 7-13.

7. Appendix

The data which are presented in this appendix were done in parallel with the other experiments included in the previous chapters but they were not discussed before in the text. Because of some important changes we found in these experiments, we decided to present them as an appendix. We believe that the information gathered suggested by these data may help to design more experiments highlighting the importance of dysbindin-1 in future.

1a: Functional effect of dysbindin-1 gene on hippocampal network oscillation

The hippocampus, in itself, is an astonishingly organized neural structure that displays a variety of synchronous oscillations under physiological or pathophysiological conditions. Brain oscillations in the theta (3-12 Hz) and gamma frequency bands (30-250Hz) are crucial for supporting normal cognitive and executive functioning. These rhythmic patterns were shown to arise in a wide range of mammals including mice (Buzsaki *et al.*, 2003) and humans (Kahana *et al.*, 1999). Theta and gamma rhythms are believed to provide a link between sensory perception and existing cognitive representations stored in the brain. These rhythmic activities are the result of subtle interactions between the population of local GABAergic interneurons and glutamatergic pyramidal cells. Although most current studies investigate the relevance of gamma oscillations to scz, theta rhythm has long been proven to be critical for episodic and working memory since abolishing theta impair these types of learning (Axmacher *et al.*, 2010). We aimed in the current experiment to assess whether the observed changes in the pre-pubertal hippocampal glutamatergic system could translate into physiological changes in hippocampal network activity.

In a recent study, our laboratory have shown for the first time the experimental conditions necessary to have normal hippocampal theta activity *in vitro* (Goutagny *et al.*, 2008). This method consists in using a complete hippocampal preparation *in vitro* which offers the unique opportunity to determine the intricate network mechanism responsible in generating theta rhythm using powerful *in vitro* techniques such as multiple intra- and extra-cellular recordings as well as precise pharmacology which are nearly impossible to perform *in vivo*.

To reach our goal, all the experiments were done using a new complete hippocampal preparation *in vitro* developed in our laboratory that exhibit spontaneous oscillations in theta range (Goutagny *et al.*, 2008). The use of this *in vitro* hippocampal preparation offers many advantages. First and in contrast to classical slices experiments, it preserves all the synaptic connections within the hippocampus. Second, it allows us to perform simultaneous extracellular and whole-cell patch recordings. Third, all the experiments can be performed free of anesthetics which are known to cause serious disturbances in firing patterns and synaptic transmission. Finally, these oscillations appear spontaneously free of pharmacological agonists typically used in classical *in-vitro* experiments.

Juvenile PD 16-21 C57BL/6J WT, *sdyl/+* and *sdyl/sdyl* mice were sacrificed by decapitation and the brains removed rapidly and placed in ice-cold “low-CaCl₂” sucrose, pH 7.4, equilibrated with 95% O₂/5% CO₂, containing (in mM): sucrose 252, NaHCO₃ 24, Glucose 10, KCl₃, MgSO₄, NaH₂PO₄, and 1.2 CaCl₂. After removal of the cerebellum and frontal part of the brain, a cut was made through the interhemispheric sulcus to separate the two hemispheres thereby exposing the hemisected septum. As described previously (Manseau *et al.*, 2005; Goutagny *et al.*, 2008), the half-septum and

hippocampus was then be carefully dissected out from each hemisphere by inserting a flat micro spatula in the lateral ventricle and sliding along the corpus callosum at both dorsal and ventral contours of hippocampus and septum. The hippocampus was separated from the half-septum at the septohippocampal fibers of the fornix/fimbria bundle and then left to rest in aCSF solution (room temperature; oxygenated (95% O₂/5% CO₂, standard CaCl₂, 2.0mM) for 1–3 h prior to the start of recordings. For all experiments, single hippocampal preparations was transferred to a fully submerged custom-made Plexiglas chamber, placed and weighted down on a nylon mesh. The recording chamber is on a stage of a microscope (American Optical 200M) enable with 5X magnification objective. The hippocampus was continuously perfused with “high-potassium” aCSF (4.0 mM KCl as opposed to 3mM) at a rate of 15-20ml/min for electrophysiological recordings and all recordings were performed between 29-31 °C. Field activity was be assessed from electrodes lowered into the tissue in stratum radiatum near the subiculum/CA1 and CA3 pyramidal layer, where both theta and gamma frequencies can be detected.

Local field potentials were down sampled and filtered to 500Hz, and the first and last second of data removed. Filtering was performed in the forward and reverse direction to eliminate phase distortions. Differences in CA1 theta frequency, power (amplitude) and oscillation strength were assessed using Matlab (version 2007A). CA1 power spectrums (amplitude) were calculated using the Welch method by averaging 2-5s periodgrams with a 50% overlap between segments.

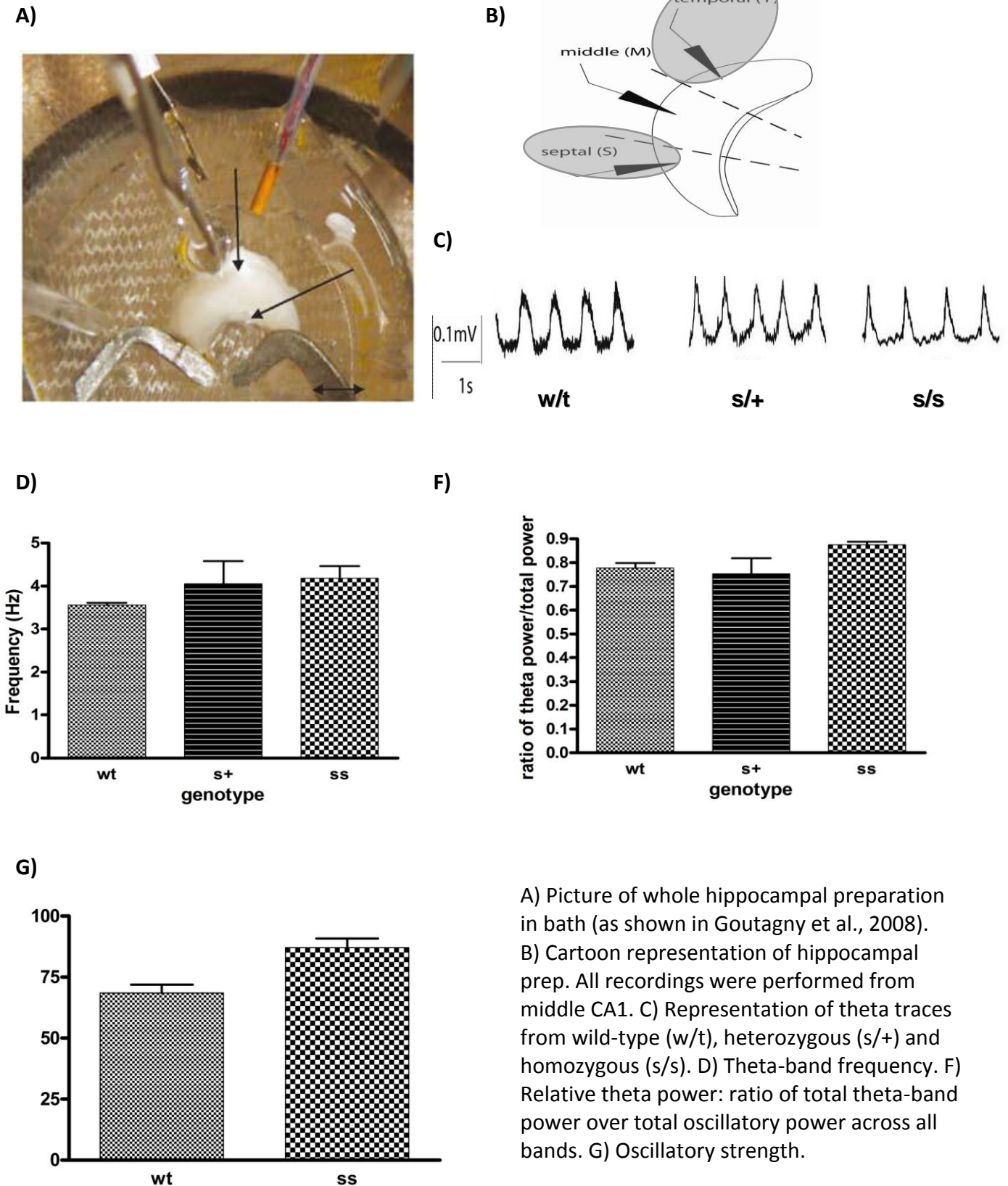
Differences between homozygous and wild-type controls were analyzed using Student’s t-test. *N* represents number of whole-hippocampal preparations. All results are expressed as mean ± SEM (as reported in figure). All statistical analyses were performed

using Prism 4 (GraphPad Software, Inc., San Diego, CA, USA). Statistical significance was defined as $p < 0.05$.

One-way ANOVA of the theta frequency power displayed no significant main effect of genotype ($F_{(2,15)} = 1.465$, $P = 0.2668$). One-way ANOVA of the relative theta power (theta power/total power across all bands) displayed significant main effect of genotype ($F_{(2,14)} = 5.655$, $P = 0.0186$). Bonferroni post-hoc analysis revealed a significant increase theta power in *sd*/*sd* as compared to wild-type ($P < 0.05$) or *sd*/*+* ($P < 0.05$). Student's two-tailed t-test on CA1 oscillation strength demonstrated a significant differences between wild-type and homozygous ($P = 0.0043$).

In summary, the present study demonstrated that although no significant changes are detected in frequency of oscillation, the *sd* hippocampal preparation appears to have higher spontaneous power and increase rhythmicity (oscillation strength). The later suggest that hippocampus from homozygous are less susceptible to change rhythmic patterns and be less plastic.

Figure 14. CA1 Theta frequency analysis



A) Picture of whole hippocampal preparation in bath (as shown in Goutagny et al., 2008).
 B) Cartoon representation of hippocampal prep. All recordings were performed from middle CA1.
 C) Representation of theta traces from middle CA1.
 D) Theta-band frequency.
 E) Relative theta power: ratio of total theta-band power over total oscillatory power across all bands.
 F) Oscillatory strength.